Chapter 2: Anion interaction and theoretical calculations of compounds **4a-h**

Anions play an important role in biological systems, environment and industrial applications. The detection of anions is generally carried out *via* two different ways: fluorescent and colorimetric sensing, were the detection is translated into a signal using a specific devise. The fluorescence detection is generally preferred over the UV-vis absorption method because of its high sensitivity. As a continuation of our work on Schiff bases of coumarin-hybrid molecules,[12,13] and to further investigate the importance of diethylamino group on the 7-position of coumarin,[4] Schiff bases **4a-h** were tested in both organic and aqueous solutions with the tetrabutylammonium salts of ten of the most common anionic analytes including CN^-, F^-, AcO^-, $H_2PO_4^-$, NO_3^-, ClO_4^-, Cl^-, Br^-, I^- and HSO_4^-. Since both the nature and position of a substituent can alter the sensing abilities of a given species, the tested compounds bear different substituents with electron donating groups in different positions and a conjugated group (Fig. 18).

Solvent effect plays also an important role in the photophysical properties of organic molecules. The present study investigates the spectral behaviors of the new Schiff bases in five different solvents with different polarities (toluene, THF, DCM, DMSO and acetic acid), then the sensing abilities towards the already mentioned anions.

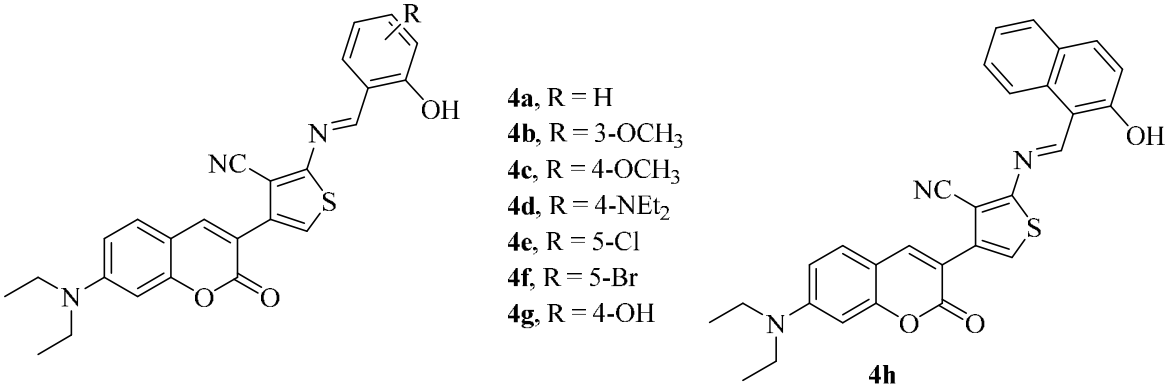

Fig. 18. Structures of compounds **4a-h**.

I. Photophysical properties of 7-diethylamino coumarin derivatives 4a-h

The 7-diethylamino coumarin derivatives **4a-h**, are non fluorescent colored substances in the solid state. Once in solution, they exhibit a yellow-green fluorescence in some solvents. The compounds are soluble in polar and non polar solvents with only some exceptions (**4f** was not soluble in acetic acid, **4g** was not soluble in toluene and **4h** in both mentioned solvents). Absorption and emission spectra (Fig. 19) were recorded at room temperature with excitation wavelengths corresponding to the maximum absorption bands. The data calculated or extracted from the spectra is presented in Table 3.

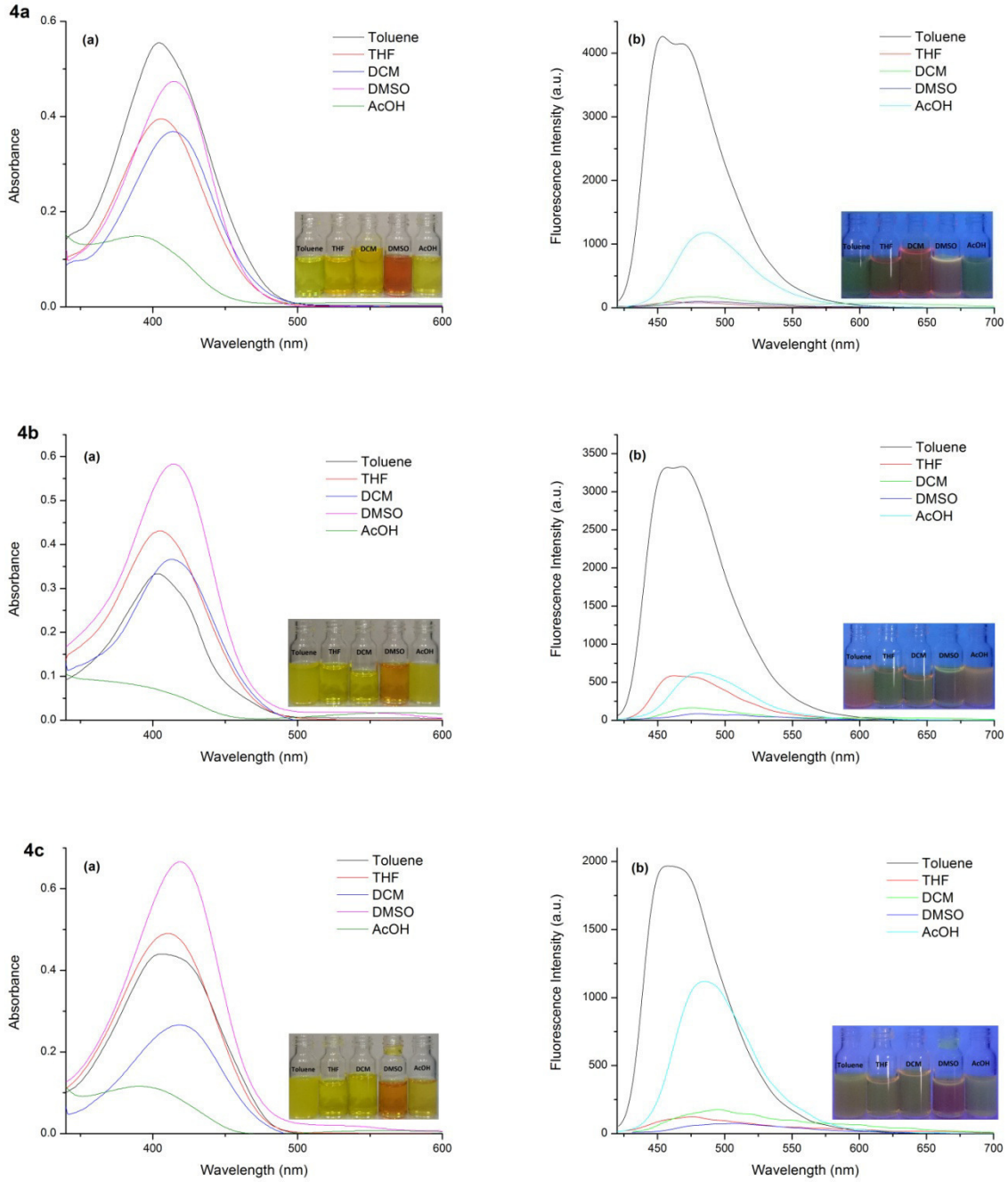

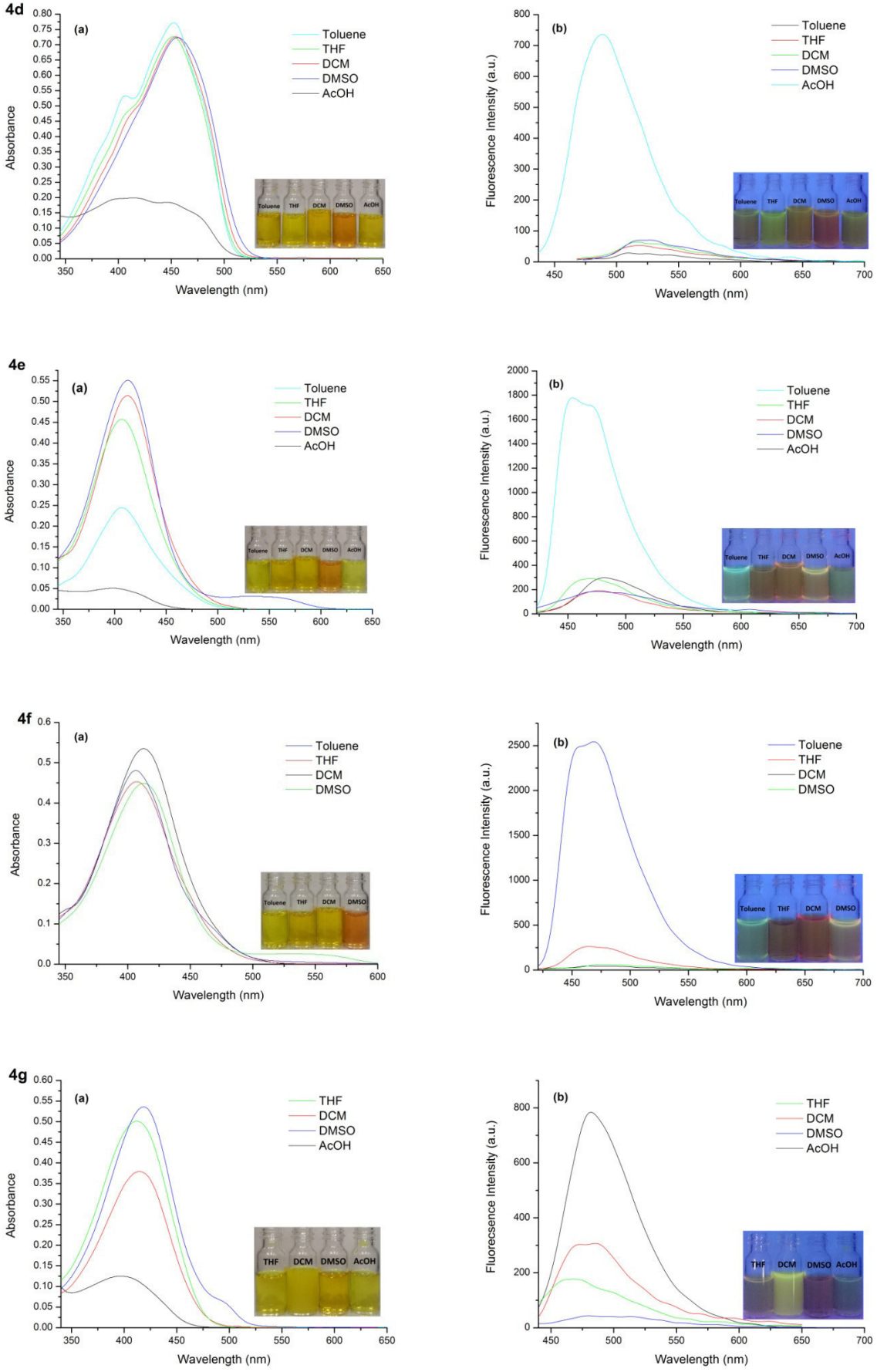
4d
(a)
Absorbance
Wavelength (nm)
Toluene
THF
DCM
DMSO
AcOH
(b)
Fluorescence Intensity (a.u.)
Wavelength (nm)
4e
(a)
Absorbance
Wavelength (nm)
(b)
Fluorescence Intensity (a.u.)
Wavelength (nm)
4f
(a)
Absorbance
Wavelength (nm)
(b)
Fluorescence Intensity (a.u.)
Wavelength (nm)
4g
(a)
Absorbance
Wavelength (nm)
(b)
Fluorecsence Intensity (a.u.)
Wavelength (nm)

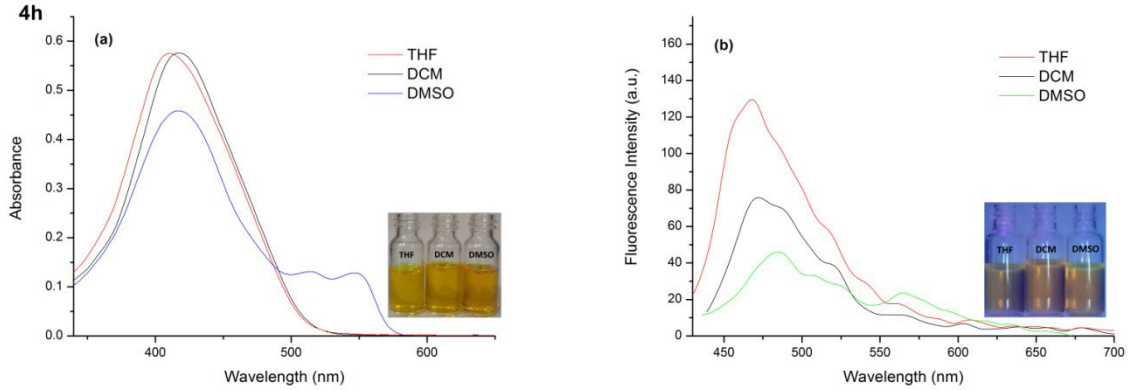

Fig. 19. (a) Absorption spectra (1×10^{-5} M); (b) Emission spectra (1×10^{-6} M) of compounds **4a**, **4b**, **4c**, **4d**, **4e**, **4f**, **4g** and **4h** in different solvents. Insets: Photographs of the solutions (1×10^{-3} M).

Table 3. Spectrophotometric properties of 7-diethylamino coumarin derivatives **4a-h**.

Solvent[a]	**4a**					**4b**				
	λ_{abs} [b]	λ_{fl} [c]	Stokes shift [d]	ε [e]	Φ_{fl} [f]	λ_{abs} [b]	λ_{fl} [c]	Stokes shift [d]	ε [e]	Φ_{fl} [f]
Toluene	404	454	50	55100	0.46	404	468	64	31300	0.60
THF	406	462	56	49500	0.01	405	462	57	40100	0.06
DCM	413	484	71	37100	0.02	414	476	62	50400	0.01
DMSO	414	480	66	59400	0.01	414	480	66	50900	0.01
Acetic acid	390	486	96	51400	0.30	404	481	77	40900	0.21
Solvent[a]	**4c**					**4d**				
	λ_{abs} [b]	λ_{fl} [c]	Stokes shift [d]	ε [e]	Φ_{fl} [f]	λ_{abs} [b]	λ_{fl} [c]	Stokes shift [d]	ε [e]	Φ_{fl} [f]
Toluene	406	458	52	52200	0.71	452	509	57	72100	<0.01
THF	409	476	67	52200	0.02	452	518	66	88600	0.01
DCM	418	495	77	44600	0.02	454	516	62	48600	0.01
DMSO	419	508	89	55600	0.01	456	527	71	66100	0.01
Acetic acid	390	485	95	39100	0.26	446	488	42	60200	0.07
Solvent[a]	**4e**					**4f**				
	λ_{abs} [b]	λ_{fl} [c]	Stokes shift [d]	ε [e]	Φ_{fl} [f]	λ_{abs} [b]	λ_{fl} [c]	Stokes shift [d]	ε [e]	Φ_{fl} [f]
Toluene	407	454	47	38800	0.26	405	469	64	46400	0.31
THF	407	470	63	65100	0.03	407	465	58	51500	0.03
DCM	412	478	66	60100	0.02	413	464	51	62200	0.01
DMSO	413	476	63	36700	0.04	413	474	61	30400	0.01

Acetic acid	398	481	83	17600	0.08	-	-	-	-	-

Solvent[a]	**4g**					**4h**				
	λ_{abs} [b]	λ_{fl} [c]	Stokes shift [d]	ε [e]	Φ_{fl} [f]	λ_{abs} [b]	λ_{fl} [c]	Stokes shift [d]	ε [e]	Φ_{fl} [f]
Toluene	-	-	-	-	-	-	-	-	-	-
THF	412	468	56	58200	0.02	410	468	58	16500	<0.01
DCM	415	485	70	33700	0.03	417	472	55	56000	0.01
DMSO	418	478	60	51700	0.01	417-519-547	485	68	50800	0.01
Acetic acid	398	482	84	50600	0.38	-	-	-	-	-

[a] In order of their increasing E_T^N values;[14] [b] long-wavelength absorption maximum, in nm; $c = 1\times10^{-5}$ M; [c] fluorescence emission maximum, in nm; $c = 1\times10^{-6}$ M; [d] Stokes shift in nm; [e] extinction coefficient, $cm^{-1}M^{-1}$; [f] fluorescence quantum yield relative to Coumarin 153 (0.38) in ethanol.

The compounds showed a close similarity in the positions of the absorption bands for all the derivatives in the series, with low absorbance values in acetic acid. The similarity is especially observed between **4a**, **4b** and **4c**, and between **4e** and **4f**. As can be seen in Fig. 16, except for compound **4h** in DMSO, the compounds showed one absorption maxima in the visible region with all the solvents, without remarkable wavelength shift (less than 14 nm) for toluene, THF, DCM and DMSO. In acetic acid, the absorption maxima of compounds **4a**, **4c**, **4e** and **4g** are blue-shifted, thus the Stokes shifts are bigger.

The emission spectra have a maximum centered between 454-527 nm. The compounds have one peak and **4a**, **4b**, **4e** and **4f** present a shoulder in toluene. Compound **4d** gave particular results, with longer absorption and emission wavelengths due to the presence of two diethylamino groups. The other compounds exhibited a very weak fluorescence in THF, DCM and DMSO ($\Phi_{fl} \leq 0.06$), slightly enhanced in acetic acid (Φ_{fl} up to 0.38), and rather good fluorescence in toluene with fluorescence quantum yield reaching 0.71 in the case of **4c**.

One remarkable feature is the presence, in addition to the main peak, of two other bands at 519 nm and 547 nm for compound **4h** in DMSO. According to previous studies,[15-18] when the Schiff bases are prepared from 2-hydrohy-1-naphthaldehyde new bands above 400 nm are observed in DMSO, EtOH, chloroform, benzene and cyclohexane. Those bands are attributed to the keto-enamine tautomeric form of the molecule (Scheme 21). The enol form has no absorbance in this region. For the Schiff bases derived from salicylaldehyde, the keto-

enamine form is not observed in those same solvents. In our case, a minor rise was detected in DMSO with **4b**, **4c**, **4e** and **4g**. The other tautomer of **4h** was not detected by ^{1}H NMR due to the very low solubility of the compound in DMSO-d_6.

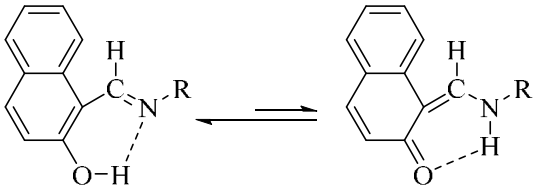

Scheme 21. Tautomerism of compound **4h**.

The photophysical results obtained, associated with the presence of a diethylamino group, made the compounds excellent candidates for their application as chemosensors.

II. Anion interaction and DFT calculations

II.1. Anion interaction

Colorometric response and interaction of the compounds in DMSO

The colorimetric analysis of the probes **4a-h** was first tested by adding the anions to a DMSO solution containing the compounds at a concentration of 1×10^{-4} M. For compound **4a** the change in color, from yellow to red (orange in the case of $H_2PO_4^-$), was immediate upon addition of only 1 equivalent of CN^-, F^-, AcO^- and $H_2PO_4^-$, while the other anions (NO_3^-, ClO_4^-, I^-, Cl^-, Br^-, HSO_4^-) did not show any color changes (Fig. 20a). For **4g** the color change of the initial solution was rather from yellow to orange (Fig. 20b). Compound **4d** showed only a slight change in the color of the main solution after addition of 1 equivalent of the four anions (Fig. 20c). The rest of the probes showed similar results as to **4a**.

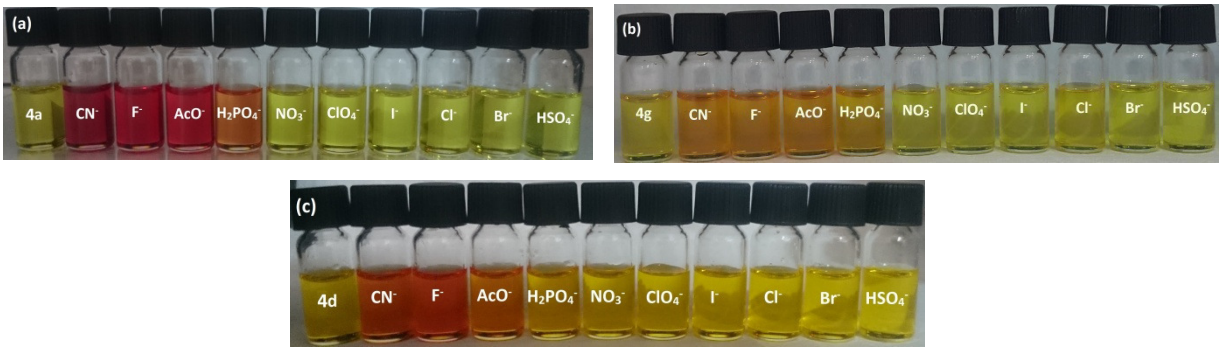

Fig. 20. Color changes of **4a** (a), **4g** (b) and **4d** (c) (1×10^{-4} M in DMSO) upon addition of 1 equiv. of different anions.

After addition of 14 equivalents to probe **4g**, no important change was observed with AcO^-, CN^- and $H_2PO_4^-$, whereas the solution of F^- turned dark red with a higher and different

fluorescence than the other anions (Fig. 21). Those changes were not observed with the other compounds after the addition of 6 equivalents of the anions.

Fig. 21. Color changes of Chemosensor **4g** (1×10^{-4} M in DMSO) upon addition of 14 equiv of different anions under ambient light (above) and UV light (below).

UV-vis and fluorometric spectra were then recorded in order to study the sensing abilities of the prepared chemosensors.

To a DMSO solution of chemosensors **4a-h** (1×10^{-5} M), 6 equivalents of each anion (CN^-, F^-, AcO^-, $H_2PO_4^-$, NO_3^-, ClO_4^-, I^-, Cl^-, Br^-, HSO_4^-) were added (14 equivalents in the case of **4g**). According to the UV-vis spectrum of probe **4a**, Fig. 22a, addition of CN^-, F^- and AcO^- anions led to the appearance of a new band at 531 nm. Slight spectral changes were observed after addition of $H_2PO_4^-$ anion and no changes with the rest, confirming the colorimetric response already discussed. The emission spectra of the interaction **4a**-anions showed also the existence of a new band at 610 nm only with CN^-, F^- and AcO^-, as expected, with a slight increase in the intensity after addition of $H_2PO_4^-$, while no changes were observed with the other anions under the same conditions. There was also an increase in the intensity of the original band at 480 nm, and this only with cyanide (Fig. 22b).

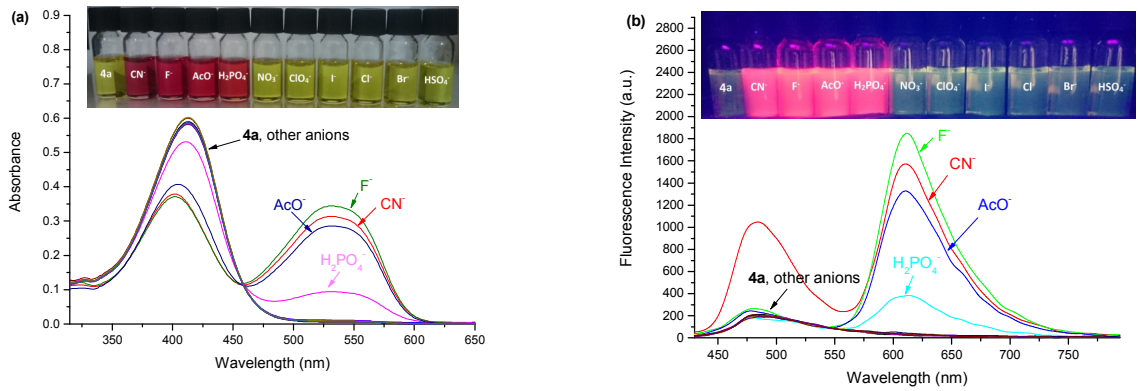

Fig. 22. (a) Absorption spectrum; (b) Emission spectrum of **4a** (1×10^{-5} M in DMSO) after addition of 6 equiv. of the anions. Insets: color and fluorescence changes after addition of 6 equiv. of anions.

Those same results were obtained with probes **4b**, **4c**, **4e** and **4f**. Indeed, the UV-vis spectra exhibited a bathochromic shift from 414, 419, 413 and 413 nm for **4b**, **4c**, **4e** and **4f**, respectively, to 535 nm for all the compounds, and this upon addition of 6 equivalents of CN^-, F^- and AcO^- anions, always with slight changes with $H_2PO_4^-$. The emission spectra showed also an emergence of a new band in the interval 580-634 nm after interaction with the anions mentioned before (Figs. A1-A4 in Annex 1).

For probe **4h**, the UV-vis spectrum recorded in DMSO showed the existence of a band at 417 nm and a smaller band at 550 nm. Addition of 6 equivalents of CN^-, F^- and AcO^- led to a hypochromic shift of the band at 417 nm, a hyperchromic shift of the band at 550 nm and a development of a new band at 520 nm, a very slight change was also observed with $H_2PO_4^-$ (Fig. 23a). The emission spectrum was rather like the other compounds, where a new band at 578 nm appeared after addition of CN^-, F^- and AcO^-, with no changes with the rest of the anions (Fig. 23b).

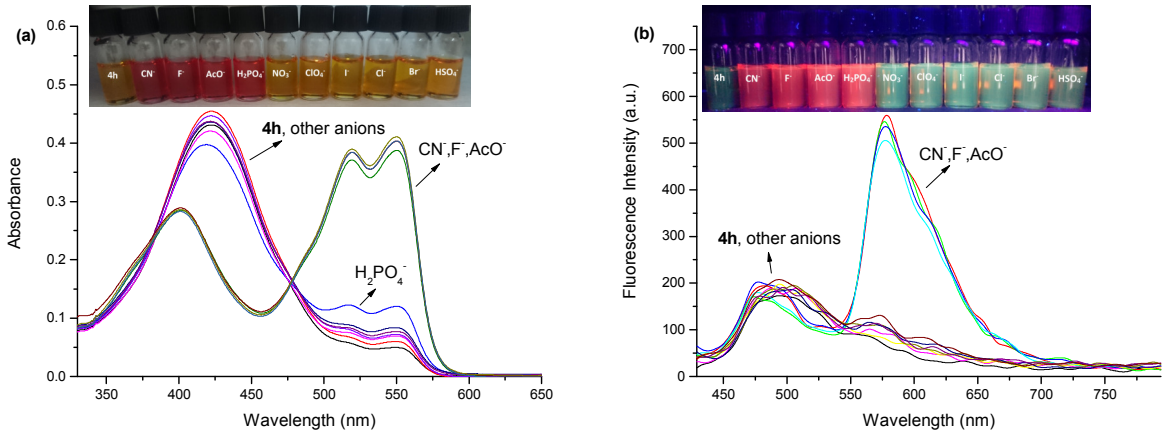

Fig. 23. (a) Absorption spectrum; (b) Emission spectrum of **4h** (1×10^{-5} M in DMSO) after addition of 6 equiv. of the anions. Insets: color and fluorescence changes after addition of 6 equiv. of anions.

On the other hand, compound **4g** gave different results, probably due to the existence of two hydroxyl groups, where a development of a new band at a shorter wavelength compared to the other compounds was rather observed. Fluoride anion exhibited a high fluorescence intensity compared to cyanide and acetate (Fig. 24b). However, the colorimetric response was not detectible by UV-vis at a concentration of 1×10^{-5} M, and all the three anions (F^-, AcO^-, and CN^-) had almost the same absorbance, $H_2PO_4^-$ gave a high absorbance and HSO_4^- showed a slight spectral change (Fig. 24a). This suggests that **4g** can detect fluoride in organic medium by a "naked-eye" experiment at high concentrations.

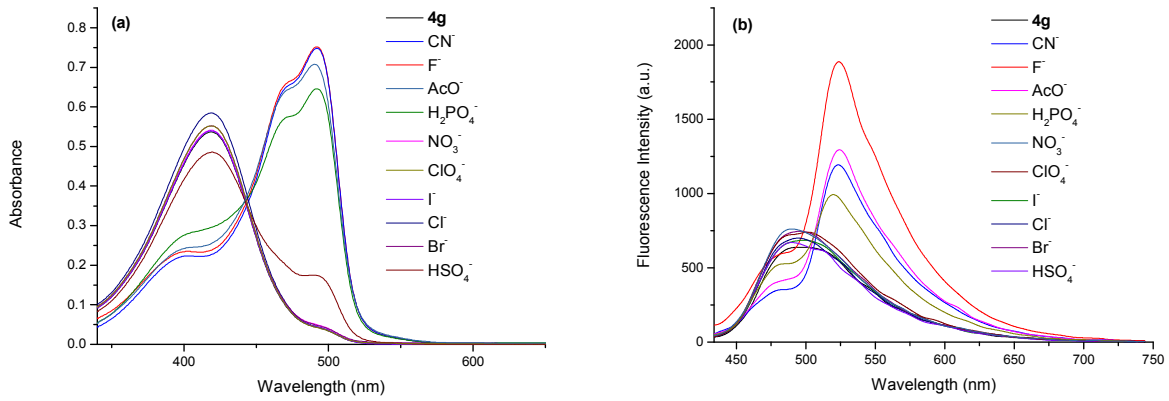

Fig. 24. (a) Absorption spectrum; (b) Emission spectrum of chemosensor **4g** (1×10^{-5} M in DMSO) after addition of 14 equiv. of the anions.

As an exception of all the probes, compound **4d** did not show a big selectivity towards the anions, with a quenching in the fluorescence intensity with fluoride (Fig. 25).

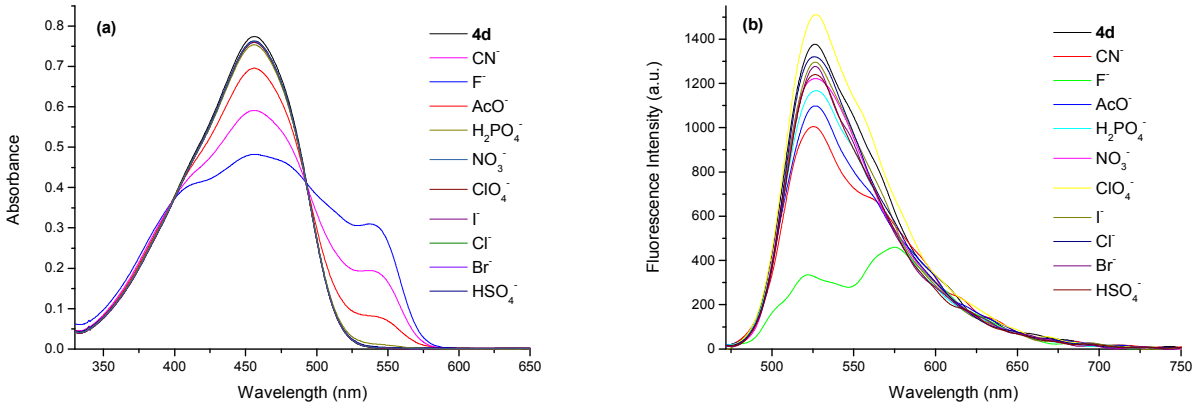

Fig. 25. (a) Absorption spectrum; (b) Emission spectrum of **4d** (1×10^{-5} M in DMSO) after addition of 6 equiv. of the anions.

Titration experiments were then carried out with cyanide, fluoride and acetate anions. The titration of chemosensor **4a** by CN^- was studied by adding increasing concentrations of the anion. As can be seen in Fig. 26a, the absorbance of the initial band at 414 nm decreased, and at the same time a new band at 531 nm developed. The existence of an isosbestic point at 460 nm indicates that the stoichiometry of the reaction remains unchanged during the interaction of the chemosensor and CN^- anion.[19] The same results were obtained with F^- and AcO^- ions (Figs. 27a, 28a). A similar study was carried out with probes **4b**, **4c**, **4e**, **4f** and **4h**. As a result, the probes gave a similar response with all the anions (Figs. A5-A17 in Annex 1).

The emission titration spectrum (Fig. 26b) of **4a** with CN^- showed a new band near the red region (610 nm) alongside an increase in the intensity of the band at 480 nm. For F^- and AcO^- titrations, there was no enhancement in the intensity of the original band at 480 nm (Figs. 27b, 28b).

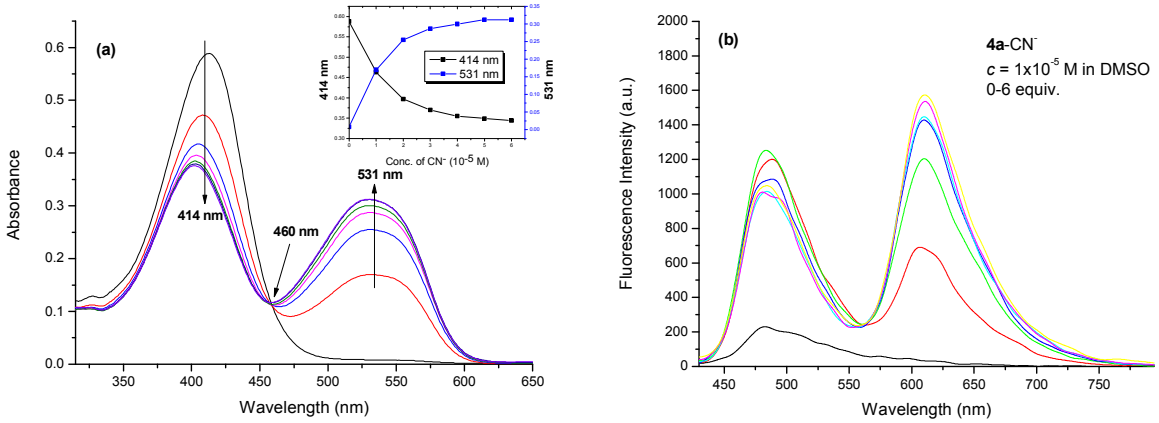

Fig. 26. UV-vis titration spectra (a) Fluorescence titration spectra (b) of chemosensor **4a** (1×10^{-5} M) with CN^- anion 0-6 equiv. in DMSO.

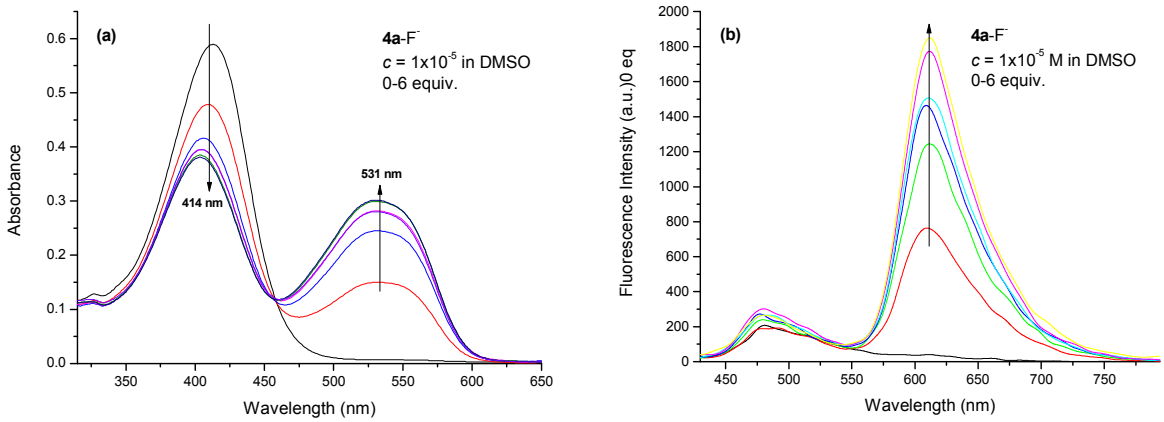

Fig. 27. UV-vis titration spectra (a) Fluorescence titration spectra (b) of chemosensor **4a** (1×10^{-5} M) with F^- anion 0-6 equiv. in DMSO.

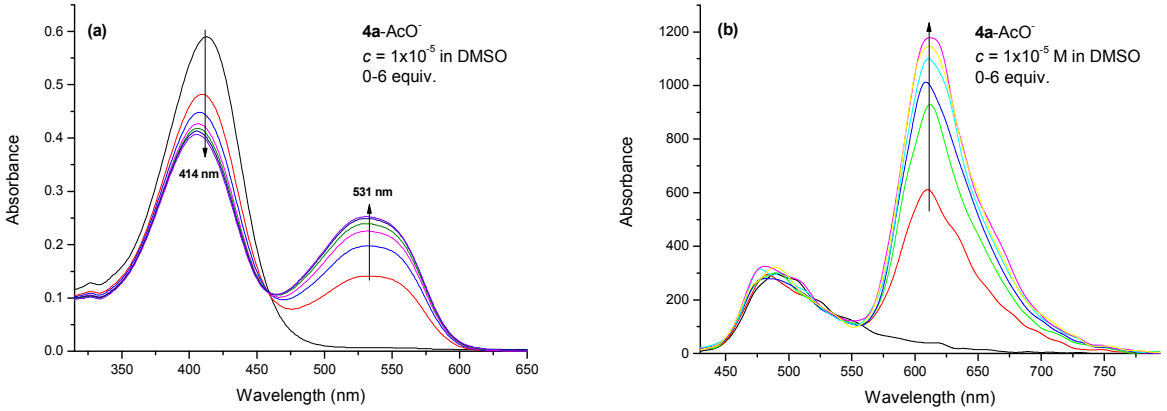

Fig. 28. UV-vis titration spectra (a) Fluorescence titration spectra (b) of chemosensor **4a** (1×10^{-5} M) with AcO^- anion 0-6 equiv. in DMSO.

Compound **4g**, upon titration with F^- anion, showed a progressive development of a new band at 492 nm (with a shoulder at 468 nm), accompanied by a hypsochromic shift of the main band at 418 nm in the UV-vis specrum (Fig. 29a). The graph also shows the appearance of an isosbestic point at 442 nm. On the other hand, the addition of increasing concentrations of F^- anion to chemosensor **4g** (1×10^{-5} M in DMSO) caused a red shift to the maximum wavelength, in the original emission spectrum (Fig. 29b). The absorbance and emission spectra of cyanide and acetate anions exhibited the same behavior as that of fluoride ion (Figs. A18, A19 in Annex 1). The study of the profile of the absorbance spectra at 492 nm showed that, the maximum absorbance was reached after adding only 5 equivalents of F^- anion.

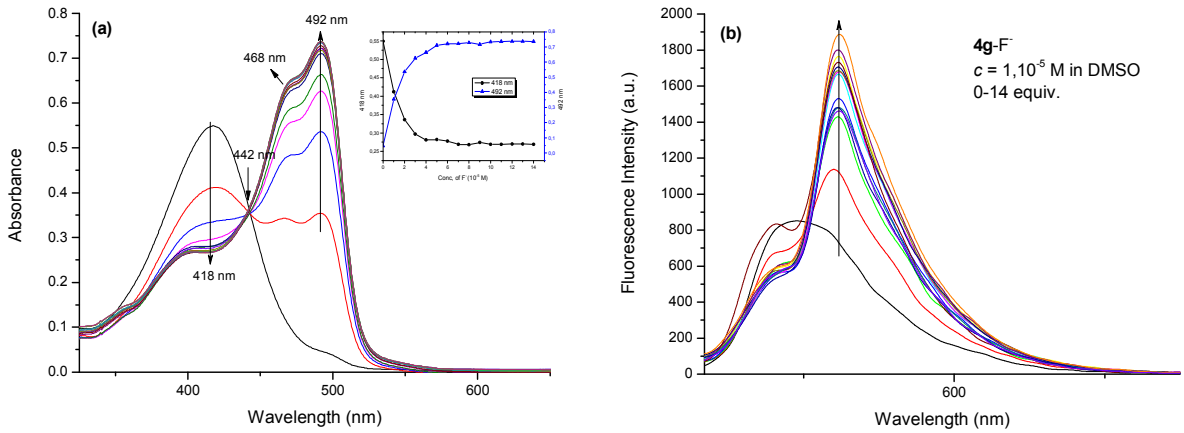

Fig. 29. UV-vis titration spectra (a) Fluorescence titration spectra (b) of chemosensor **4g** (1×10^{-5} M) with F^- anion 0-14 equiv. in DMSO.

Studies in partial aqueous media

In order to mimic a real environment, a study in a DMSO/H_2O medium was carried out. The interaction of **4g** with cyanide, fluoride and acetate was first studied in nine DMSO/H_2O binary solutions varying from 9/1 to 1/9 (DMSO/H_2O v/v). The best response in terms of UV-vis and fluorescence spectra, was obtained in the system DMSO/H_2O (6/4 v/v). Therefore, the following work was carried out in this binary solution.

Unlike what was obtained in organic medium, the interaction of the probes in aqueous solution, with the different anions employed in this study, showed a selectivity towards CN^- ion only, while the other competing anions (F^-, AcO^-, $H_2PO_4^-$, NO_3^-, ClO_4^-, I^-, Cl^-, Br^-, HSO_4^-) exhibited no changes after the addition of the same equivalents of each anion, in both UV-vis and fluorescence spectra, even the ones interacting with the probe in DMSO (F^-, AcO^- and $H_2PO_4^-$). As can be seen in Fig. 30, for probe **4a**, only CN^- responded, in aqueous medium, by a shift in the absorbance and a great increase in the fluorescence intensity, while the other anions did not show any changes in the spectral properties. The bathochromic shift in the absorbance maxima in the UV-vis spectrum, caused by the addition of CN^-, was much clearer with Chemosensor **4g** (Fig. 31).

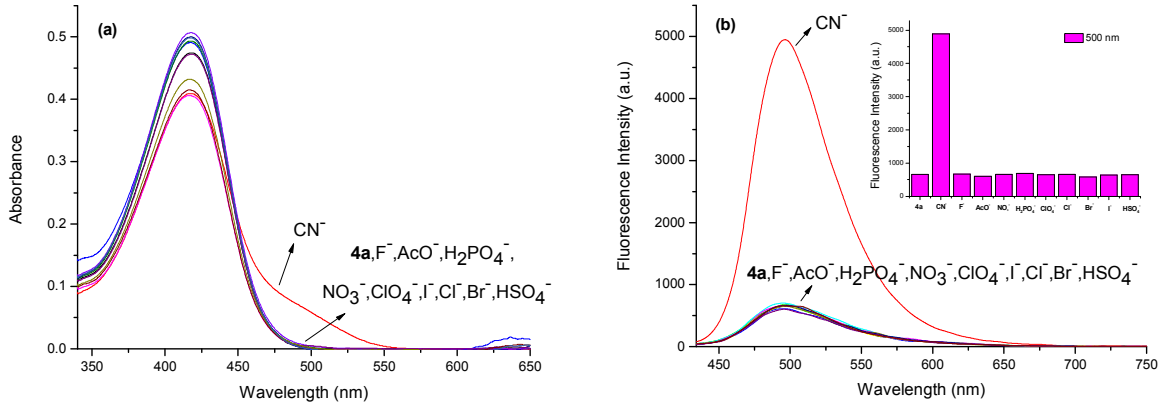

Fig. 30. (a) Absorption spectra of **4a** (10^{-5} M in DMSO/H_2O: 6/4) (b) Emission spectra of **4a** (5×10^{-6} M in DMSO/H_2O: 6/4) after addition of 20 equiv. of all the anions. Inset shows the emission intensity at 500 nm vs. various anions.

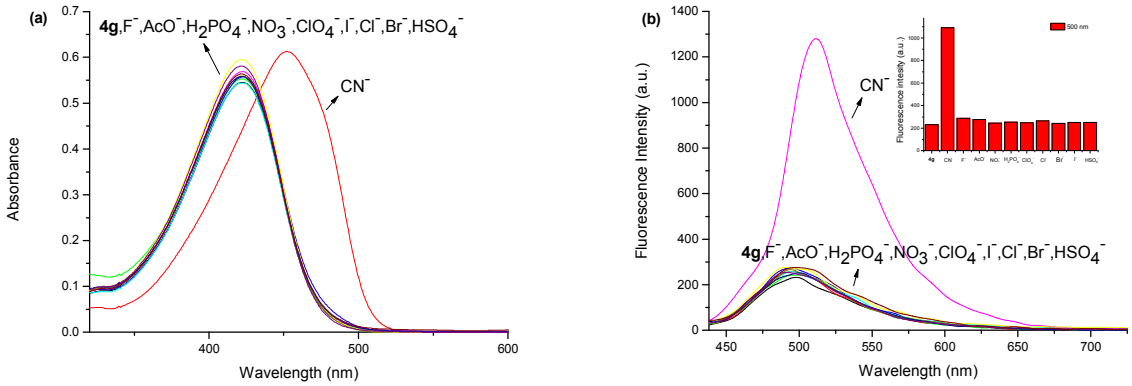

Fig. 31. (a) Absorption spectra of chemosensor **4g** (1×10^{-5} M in DMSO/H_2O: 6/4) (b) Emission spectra of chemosensor **4g** (5×10^{-6} M in DMSO/H_2O: 6/4) after addition of 14 equiv. of all the anions. Inset shows the emission intensity at 500 nm vs. various anions.

Those results are probably due to the fact that CN^- anion has low hydration energy, whilst the basicity of the other anions is significantly decreased due to the formation of hydrogen bond between the anions and water molecules.

Titration experiments were also carried out by a stepwise addition of cyanide anion. As shown in Fig. 32a, chemosensor **4a** shows an absorption band at 418 nm in DMSO/H_2O (6/4: v/v) solution. The addition of 20 equivalents of CN^- led to a change in the spectrum illustrated by the appearance of a new band at 495 nm along with a decrease in the band at 418 nm (a bathochromic shift of 77 nm, with an isosbestic point at 449 nm).

The fluorescence titration spectrum (Fig. 32b) shows that the sensor has weak fluorescence at 500 nm (λ excitation 418 nm). A strong enhancement in the intensity of the fluorescence was observed upon gradual addition of CN^- and reaches its maximum after 20 equivalents. As well as the fluorescence color of the solution becomes green with addition of CN^- anion (Inset Fig. 32b).

The UV-vis titration of chemosensor **4g** was also evaluated in aqueous solution by adding increasing concentrations of CN^- anion. As shown in Fig. 33a, the band with the maximum absorbance at 422 nm decreased, and a new band at 452 nm emerged with an isosbestic point at 432 nm. The addition of cyanide led to a change in color from light yellow to dark yellow with a considerable increase in the fluorescence intensity (Fig. 33b).

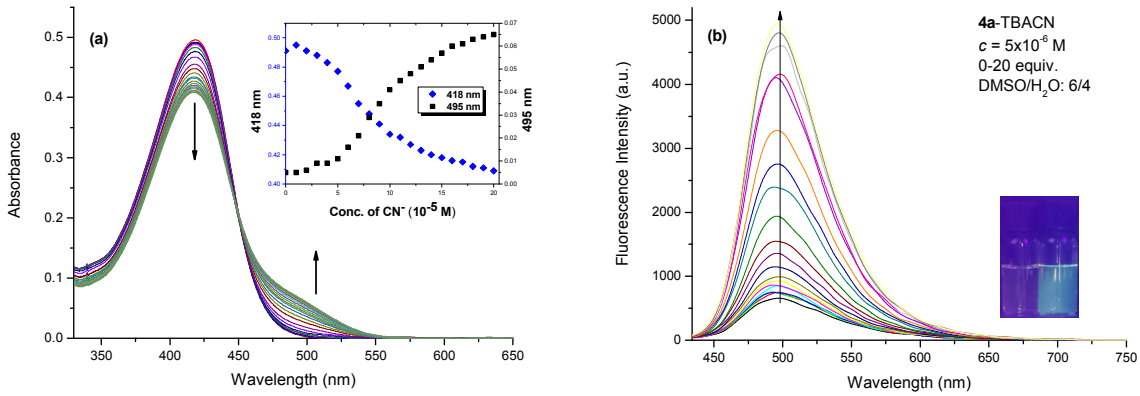

Fig. 32. (a) Absorption titration spectra of **4a** with cyanide (1×10^{-5} M in DMSO/H_2O: 6/4). Inset shows the change in absorbance at 418 and 495 nm with various concentrations of CN^- anion. (b) Emission titration spectra of **4a** with cyanide (5×10^{-6} M in DMSO/H_2O: 6/4) upon addition of 20 equiv. Inset: photograph of **4a** (1×10^{-5} M) in DMSO/H_2O (6/4, v/v) with 20 equiv. of TBACN under UV lamp.

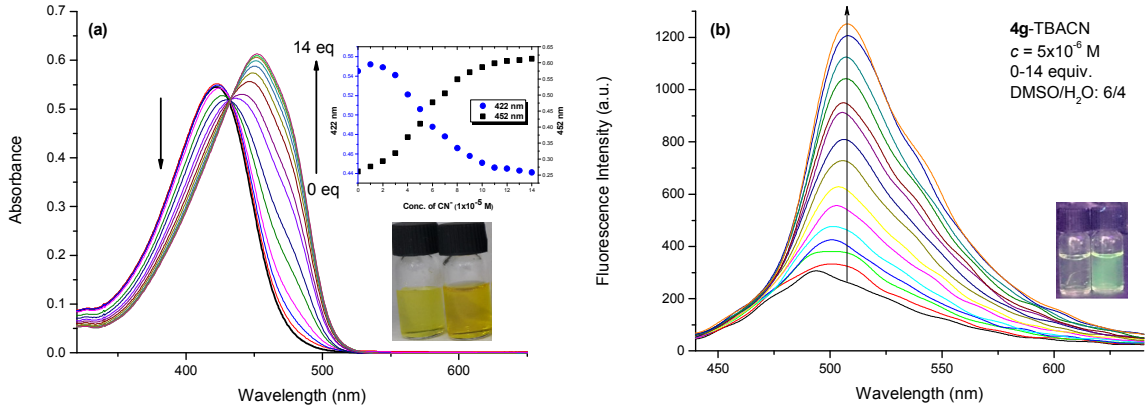

Fig. 33. (a) Absorption titration spectra of **4g** with cyanide (1×10^{-5} M in DMSO/H_2O: 6/4). Inset shows the change in absorbance at 422 and 452 nm with various concentrations of CN^- anion. (b) Emission titration spectra of **4g** with cyanide (5×10^{-6} M in DMSO/H_2O: 6/4) upon addition of 14 equiv. Inset: photograph of **4g** (1×10^{-5} M) in DMSO/H_2O (6/4, v/v) with 14 equiv. of TBACN under UV lamp.

The stoichiometry of the interaction of chemosensor **4g** with cyanide was determined using Job's plot conducted by a UV-vis experiment in DMSO.[20] The graph is a plot of the absorbance of the solution against the mole fraction ([Chemosensor]/[Chemosensor]+[CN^-]). The maximum absorbance corresponds to a fraction of 0.44, indicating a 1:1 stoichiometric ratio for complexation of the probe with CN^- (Fig. 34). Those results were further confirmed by ^{1}H NMR and IR titration experiments.

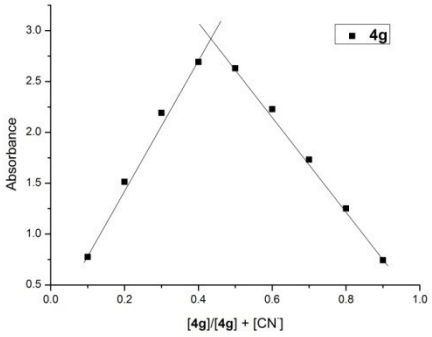

Fig. 34. Job's plot of complexation of probe **4g** (491 nm) with CN^- determined by UV-vis experiments in DMSO.

These changes (the bathochromic shifts in the UV-vis spectra and the increase of the fluorescence intensity) are due to the intramolecular charge transfer (ICT) process.[21,22] Indeed, the conjugation of the system is strengthened and the ICT efficiency is increased resulting in a red shift in the absorption spectra, accompanied by a strong enhancement in the fluorescence intensity. For probe **4g** for example, this ICT mechanism is a consequence of a di-deprotonation of the two –OH protons (Scheme 22), as deduced from the results of NMR titrations (discussed later) and also from Job's plot experiment, were a 1:1 stoichiometry was determined.

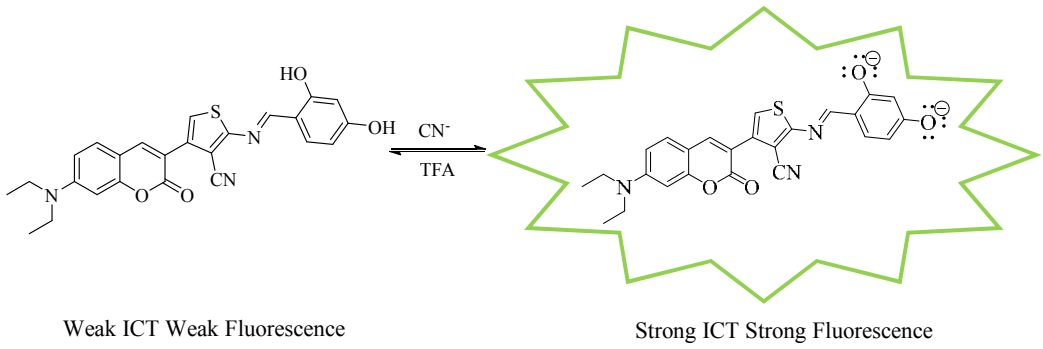

Scheme 22. Di-deprotonation process.

^{1}H NMR and IR titration experiments of chemosensor 4a and 4g

In order to clarify the mechanism of the interaction of **4a** with F^-, AcO^- and CN^-, ^{1}H NMR spectroscopy was investigated. While F^- and AcO^- gave almost the same response with **4a**, a different mechanism was encountered with CN^-.

DMSO-d_6 solution of **4a** was titrated with F^- and AcO^- up to 4 equiv. (Figs. 35, 36). Within addition of 1 equiv. of the anions, OH signal disappeared, upfield shifts of imine (He), thiophene (Hf) and phenyl protons (Ha, Hb, Hc and Hd) ($\Delta\delta$=20-60 Hz) were observed. Most

significant shifts were those of Ha and Hc signals, at the *ortho* and *para* positions of the OH group, which indicates deprotonation of OH proton that causes the change of the electron distribution in the conjugated system. As expected no significant change was observed with the coumarin ring signals. Further addition of anions (4 equiv.) did not produce any significant changes in the spectrum, except, a new peak as triplet at 16.15 ppm (114.7 Hz) appeared with addition of fluoride, indicating the formation of [HF_2^-] species.

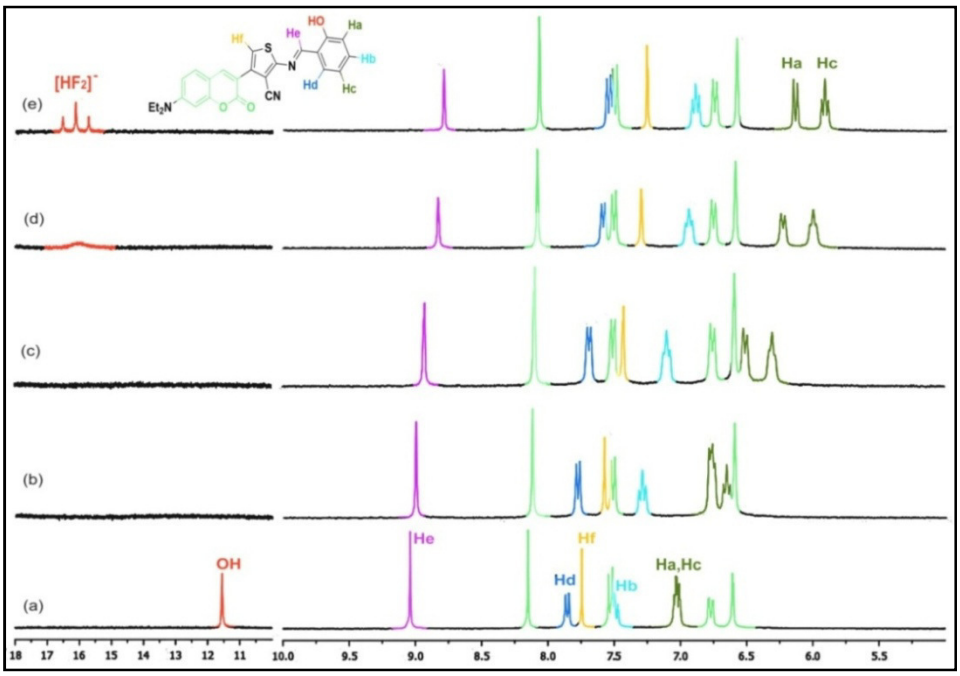

Fig. 35. ^{1}H NMR spectral change of **4a** (10 mM) in the absence (a) and presence of 1 equiv. (b), 2 equiv. (c), 3 equiv. (d) and 4 equiv. (e) of TBAF in DMSO-d_6

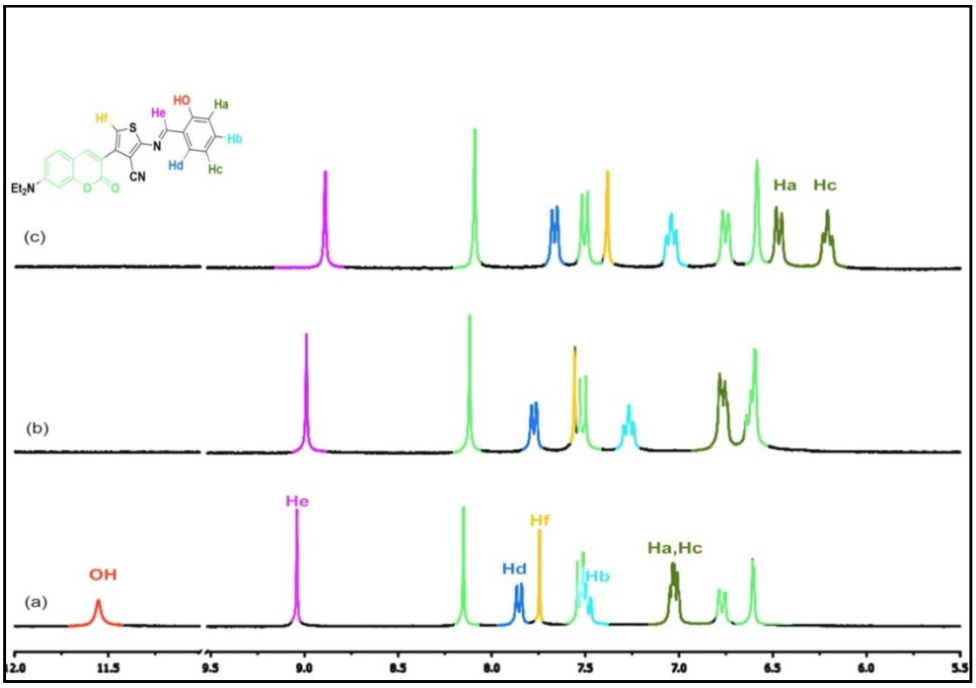

Fig. 36. ^{1}H NMR spectral change of **4a** (10 mM) in the absence (a) and presence of 1 equiv. (b) and 4 equiv. (c) of TBAAcO in DMSO-d_6

DMSO-d_6 solution of **4a** was also titrated with CN^- up to 3 equiv. (Fig. 37). Within addition of 1 equiv. of CN^-, OH signal disappeared, and all the other signals shifted slightly to upfield with an apparation of a new signal at 5.44 ppm. While NMR titration was continued up to 3 equiv. of CN^-, imine proton (He) at 9.04 ppm was mostly diminished, more importantly a new peak at 5.24 ppm appeared attributed to the addition of cyanide to the imine carbon (He') (Scheme 23). Unlike fluoride and acetate titration results, thiophene (Hf) proton and phenyl protons (Ha, Hb, Hc and Hd) showed more significant upfield shifts. Interestingly, all coumarin ring proton signals shifted to upfiled. All this changes in the chemical shifts of the signals suggest that two different mechanisms (deprotonation and addition) take place at the same time.

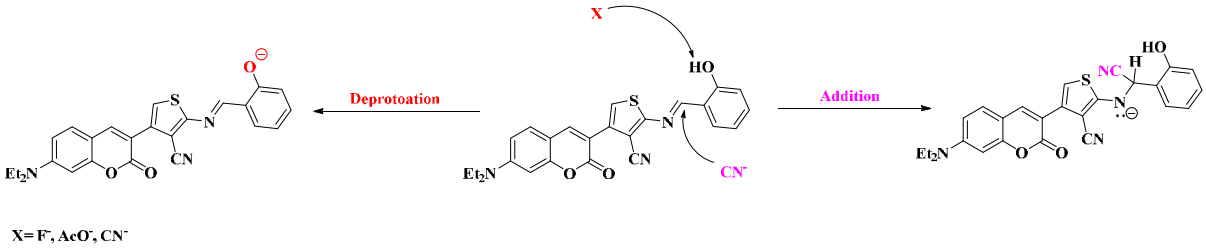

Scheme 23. Mechanism for anion interaction with sensor **4a**.

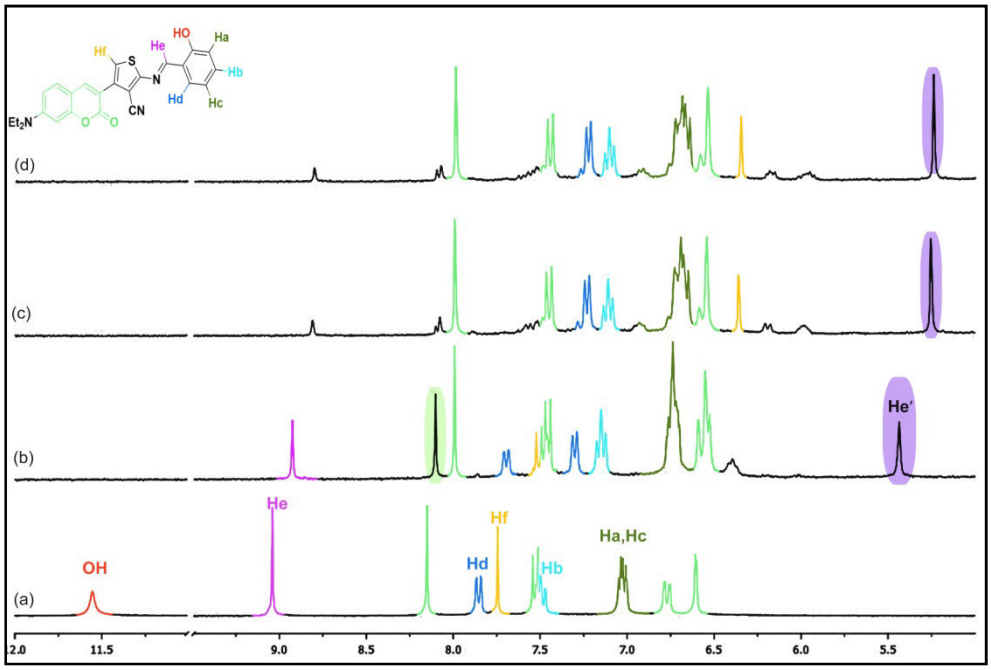

Fig. 37. ^{1}H NMR spectral changes of **4a** (10 mM) in the absence (a) and presence of 1 equiv. (b), 2 equiv. (c) and 3 equiv. (d) of TBACN in DMSO-d_6

^{1}H NMR spectroscopy was also conducted with **4g** in the presence of F^-, CN^- and AcO^-. Upon addition of 1 equiv. of the three anions, the OH protons (at 10.64 and 11.91 ppm) disappeared. The phenyl ring protons (Ha, Hb and Hc), imine proton (Hd), and the thiophene

proton signals were shifted to upfield due to an overall change of the electron distribution, which was caused by deprotonation of the OH protons. As was expected, no significant change was observed at the coumarin ring signals (Figs. 38-40). After addition of 5 equiv. of the three anions, there was no significant shift. However, upon addition of F^-, a new peak appeared which indicates the formation of a stable bifluoride anion, $[HF_2]^-$. Also, a maximum chemical shift of signals was observed with the addition of F^- anion (Fig. 41). The study of ^1H NMR spectroscopy indicates that, the mechanism involves the deprotonation of hydroxyl groups on the phenyl part of the Schiff base which was further investigated using IR titration experiments. This result is probably due to the presence of two hydroxyl groups on the aromatic ring which induced a mesomeric donor effect, and therefore made it difficult for an addition reaction to occur. Changes in chemical shifts as a result of the interaction of **4g** with F^-, AcO^- and CN^- are summarized in Table 4.

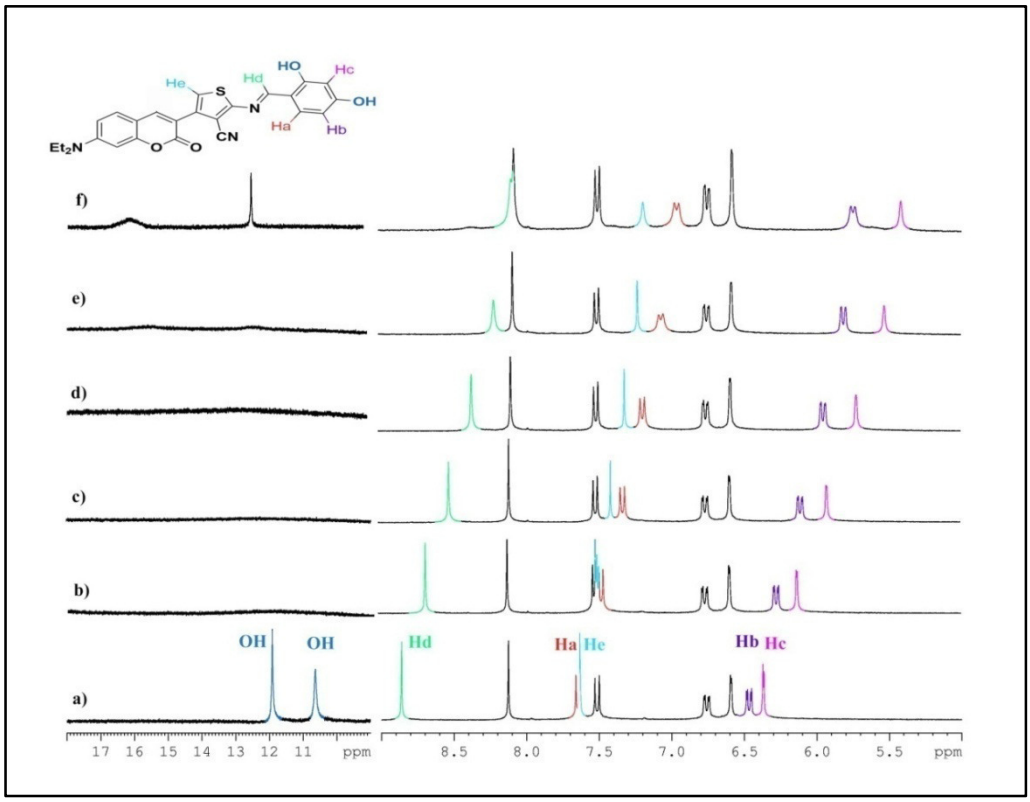

Fig. 38. Partial ^1H NMR spectra obtained *via* titrations of **4g** (1×10^{-2} M) with different amounts of TBAF solution (1 M) in DMSO-d_6. (a) **4g**; (b) 5 µL; (c) 10 µL; (d) 15 µL; (e) 20 µL and (f) 25 µL TBAF.

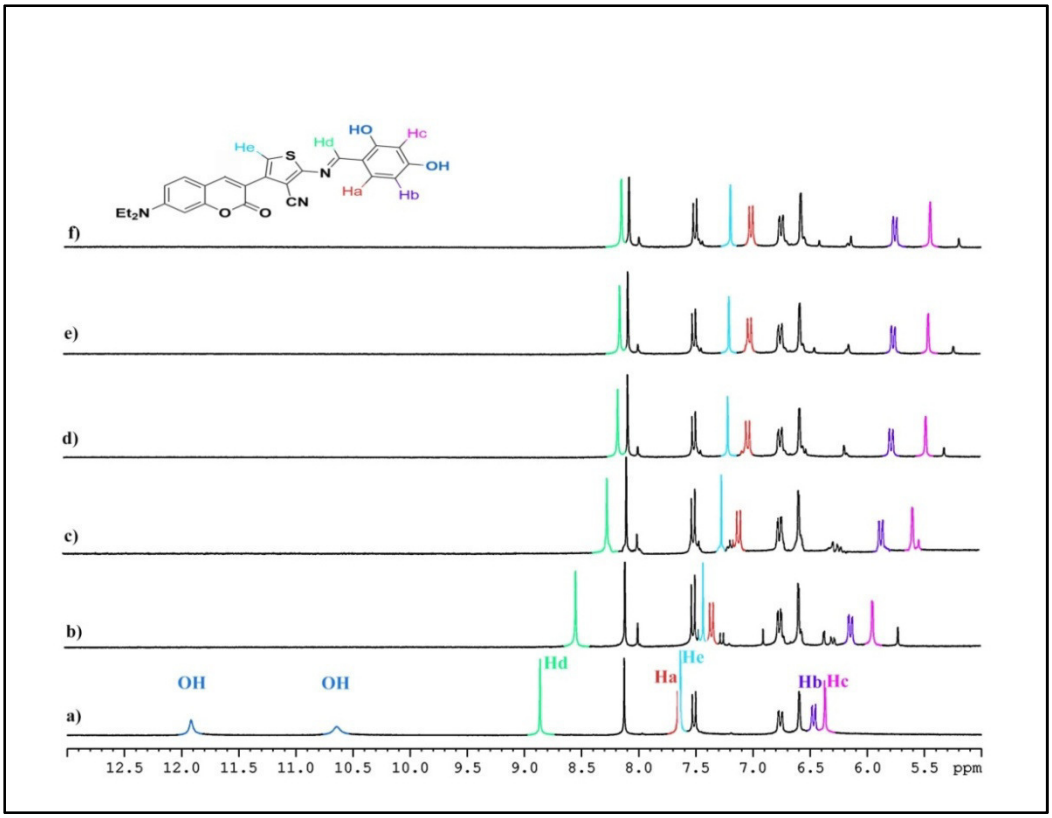

Fig. 39. Partial ^{1}H NMR spectra obtained *via* titrations of **4g** (1×10^{-2} M) with different amounts of TBACN solution (1 M) in DMSO-d_6. (a) **4g**; (b) 5 µL; (c) 10 µL; (d) 15 µL; (e) 20 µL and (f) 25 µL TBACN.

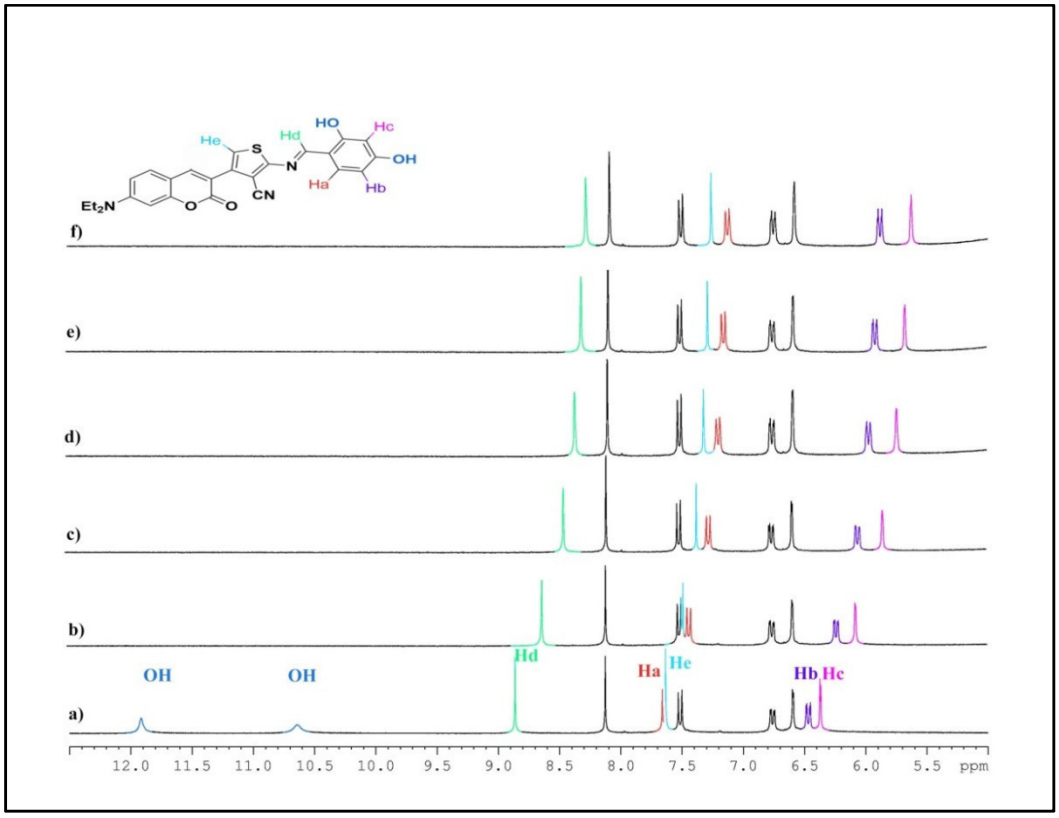

Fig. 40. Partial ^{1}H NMR spectra obtained *via* titrations of **4g** (1×10^{-2} M) with different amounts of TBAAcO solution (1 M) in DMSO-d_6. (a) **4g**; (b) 5 µL; (c) 10 µL; (d) 15 µL; (e) 20 µL and (f) 25 µL TBAAcO.

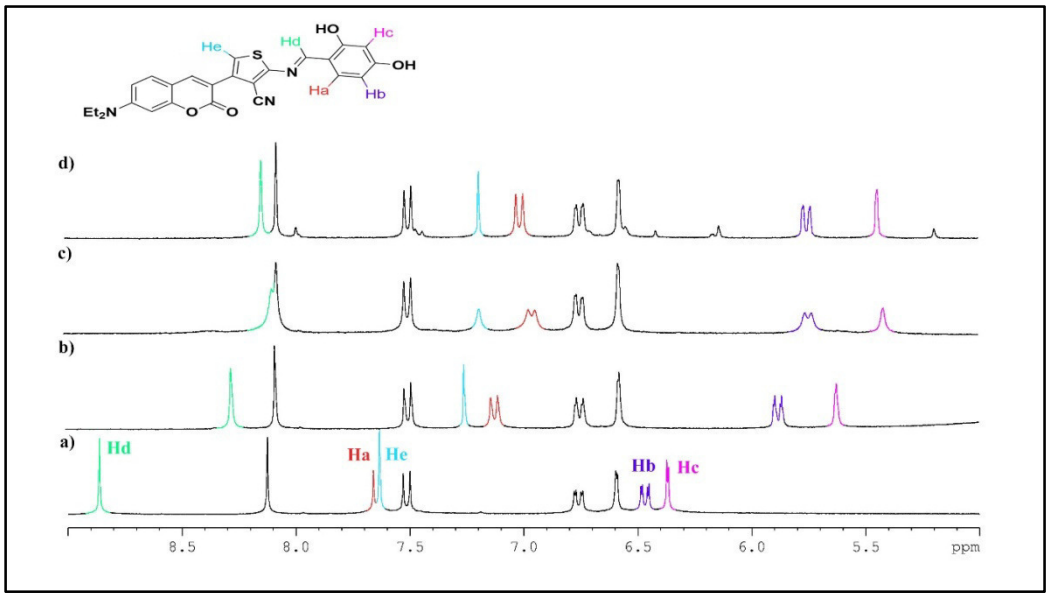

Fig. 41. Partial ^{1}H NMR spectra obtained *via* titrations of a) **4g** with b) TBAAcO, c) TBAF and d) TBACN solution (5 equiv) in DMSO-d_6.

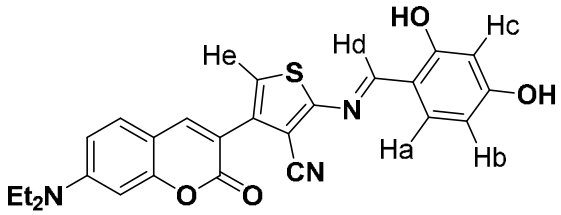

Table 4. Changes in chemical shifts as a result of the interaction of **4g** with AcO^-, CN^-, and F^-

	Ha	Hb	Hc	Hd	He
4g	7.65	6.45	6.37	8.86	7.65
AcO^-	7.13	5.88	5.62	8.28	7.25
CN^-	7.00	5.75	5.44	8.14	7.19
F^-	6.95	5.75	5.42	8.09	7.18

The evaluation of IR titrations of compound **4g** reveals a deprotonation process upon addition of CN^- and F^- ions. The spectrum of probe **4g** was first recorded in DMSO (100 µM). The subsequent addition of 14 equiv. of TBACN and TBAF separately led to the disappearance of the large band at 3357-3590 cm^{-1} corresponding to O-H groups, in both spectra (Fig. 42).

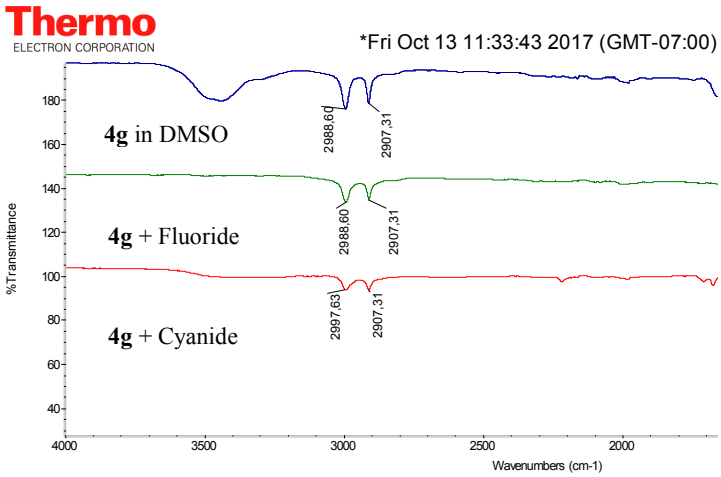

Fig. 42. IR titrations of chemosensor **4g** in the presence of 14 equiv. of F^- and CN^- anions in DMSO.

Substituent effect on anion sensing

The anion interaction with the rest of the probes was also investigated. Compounds **4b**, **4e** and **4f** showed very good selectivity towards CN^- anions, like probe **4a**, and were insensitive to all the other tested anions (F^-, AcO^-, $H_2PO_4^-$, NO_3^-, ClO_4^-, I^-, Cl^-, Br^-, HSO_4^-) as depicted in the spectra (Fig. 43). Indeed, the fluorescence intensity at around 500 nm of the mentioned probes increased dramatically upon addition of CN^- anion. Compound **4h** was also selective towards cyanide anion but with moderate fluorescence intensity. The titration experiments were also carried out, the spectra can be found in Annex 1 (Fig. A20-A23).

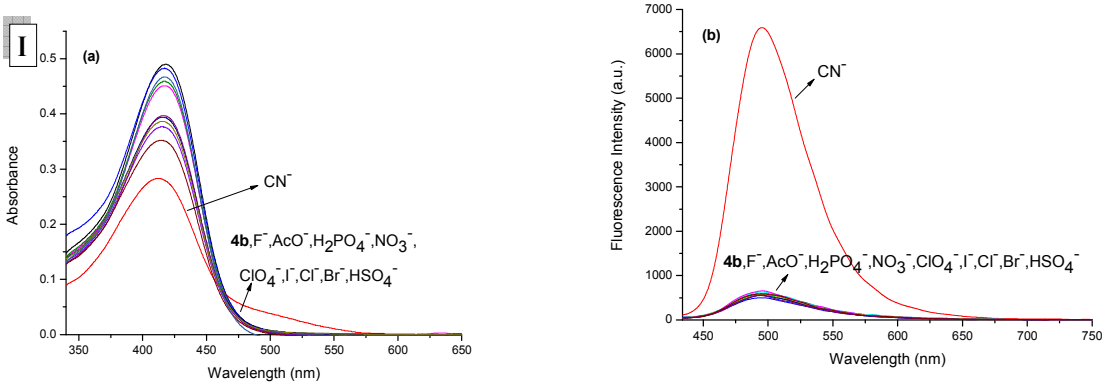

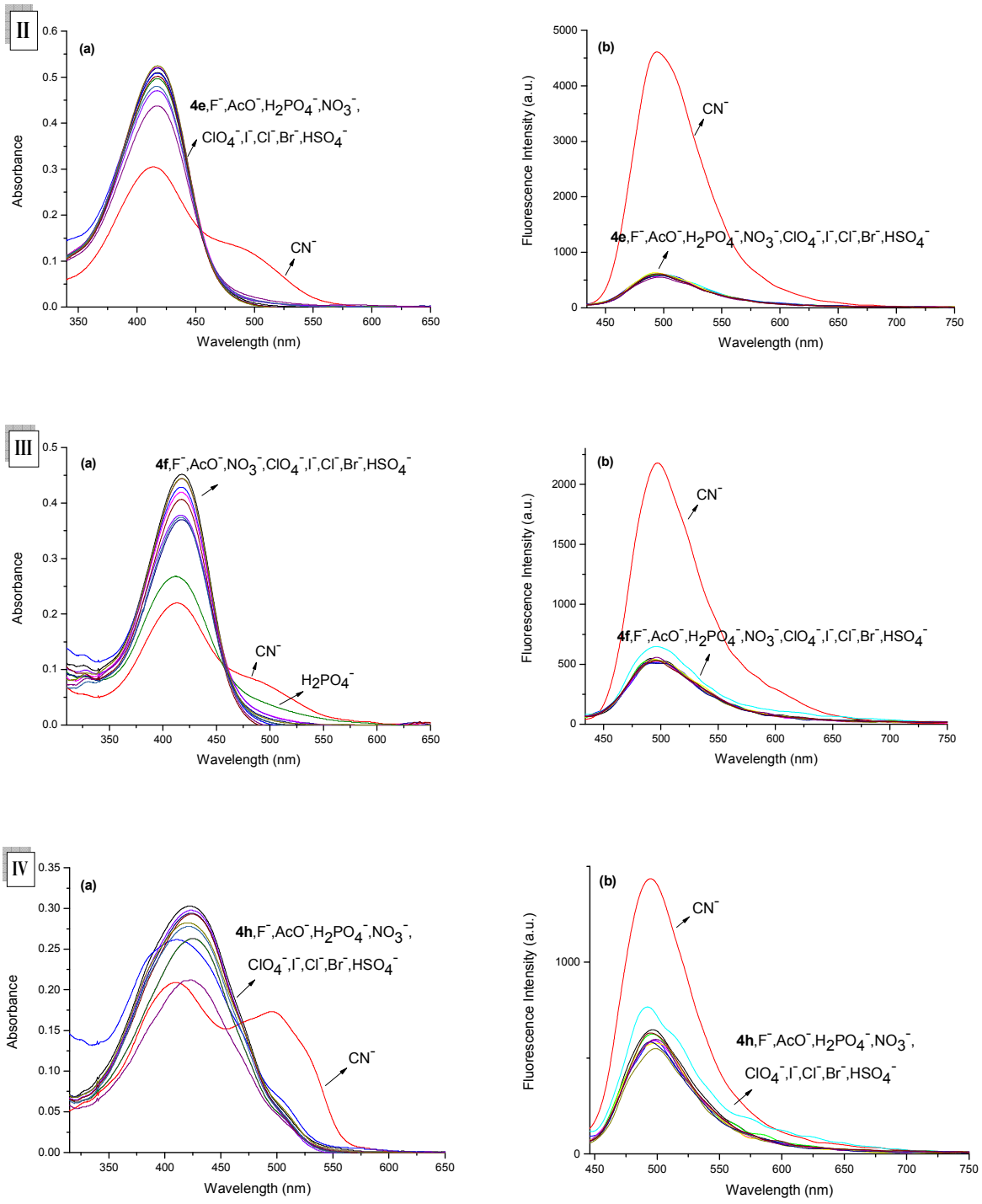

Fig. 43. (a) Absorption spectra (1×10^{-5} M in DMSO/H_2O: 6/4); (b) Emission spectra (5×10^{-6} M in DMSO/H_2O: 6/4) of (I) **4b**, (II) **4e**, (III) **4f**, (IV) **4h** after addition of 24, 28, 16 and 25 equiv., respectively, of all the anions.

The position and the electron property of the substituents affect the sensing ability of a given compound. Previous studies showed that the addition of substituents on molecules at different positions and with different donating or withdrawing characteristics affects directly the selectivity and the signaling of these compounds.[23-27] In this work we attempt an

investigation on how the addition of different functional groups on compound **4a** affects the sensing of anions.

While all the sensors prepared showed a good selectivity towards CN^- anion in partial aqueous medium, the Schiff bases prepared from salicylaldehyde bearing an electron donating group at the 4-position **4c** (with a methoxy group) and **4d** (with a diethylamino group) did not interact with any anion even cyanide.

It is well known that, the position and the electron property of the substituents of this kind of compounds change the acidity of the OH proton and the resonance of the whole conjugated system, and since the mechanism of the interaction involves both a deprotonation and an addition, the sensing ability changes dramatically. Thus, the Schiff bases prepared from salicylaldehyde bearing an electron donating group at the 4-position (**4c** and **4d**) did not interact with any anion even cyanide. It is worth noting that compound **4c** has an excellent interaction with CN^-, F^- and AcO^- anions in DMSO, while **4d** have almost no interaction, this can be explained by the fact that dialkylamino is a better donating group than methoxy.

As mentioned before, the position of the same substituent plays also a crucial role in the sensing ability of a given compound. This was displayed by compounds **4b** and **4c**, both having a methoxy group (Fig. 44), where the first gave a very good selectivity towards cyanide while the second was insensitive to all the tested anions.

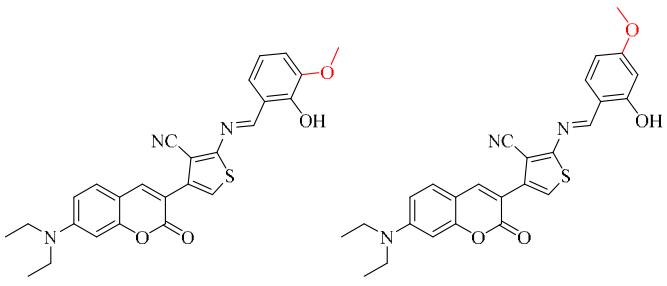

Fig. 44. Compounds **4b** and **4c**.

At the end we can deduce the following:

- The insertion of functional groups in compound **4a** affects its anion sensing abilities.
- ^1H NMR titration showed that the interaction of compound **4a** follows a deprotonation mechanism with F^- and AcO^- anions, and both a deprotonation and an addition mechanisms with CN^- anion. It is suggested that compounds **4b**, **4e**, **4f** and **4h** have the same interactions with the three anions.

- Introducing a hydroxyl group into the 4-position of the salicylidene moiety (probe **4g**) led to a di-deprotonation with no addition to the C=N double bond, while the introduction of more electrodonating groups like methoxy and diethylamino (**4c** and **4d**, respectively) tuned off the response so neither a deprotonation nor an addition took place.
- Compounds **4e** and **4f** with Cl and Br showed desirable sensing abilities and a good selectivity to cyanide.
- Varying the position of an electron donor group (methoxy), led to a change in the sensing of the molecules.
- The results obtained prove that probes **4a**, **4b**, **4e**, **4f**, **4g** and **4h** have a very good selectivity towards CN^- in partial aqueous medium.

To further test the selectivity of the probes towards CN^-, a competitive experiment was performed by mixing all the anions and CN^- ion in the same solution of probes **4b**, **4e** and **4g** (5×10^{-6} M in DMSO/H_2O: 6/4). The results prove that, even in the presence of highly competitive anions such as F^- and AcO^-, the addition of cyanide increases the fluorescence intensity (Fig. 45).

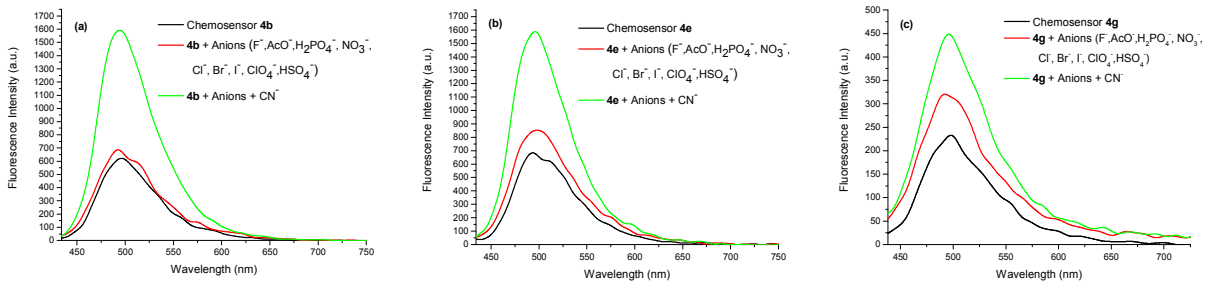

Fig. 45. The fluorescence responses of (a) **4a**, (b) **4e** and (c) **4g** (5×10^{-6} M) upon addition of 24, 28 and 14 equiv. of CN^- respectively and all the other anions in DMSO/H_2O: 6/4 (v/v).

Study of the reversibility of the interaction probe-cyanide

Given that the mechanism of the interaction host-guest involve a deprotonation process (as confirmed by ^1H NMR titration experiments), TFA was added to a solution probe-CN^-, in DMSO, in order to study the reversibility of the chemosensors.[12]

As depicted in Fig. 46, addition of 4 equiv. of TFA to a solution of **4a** containig 4 equivalents of TBACN led to a hypochromic shift of the band at 531 nm in the UV-vis spectra with the restoration of the absorbance at 414 nm and the color of the solution (from pink to

yellow). This indicates that the interaction of the probe **4a** with cyanide anion can be reversed by adding TFA.

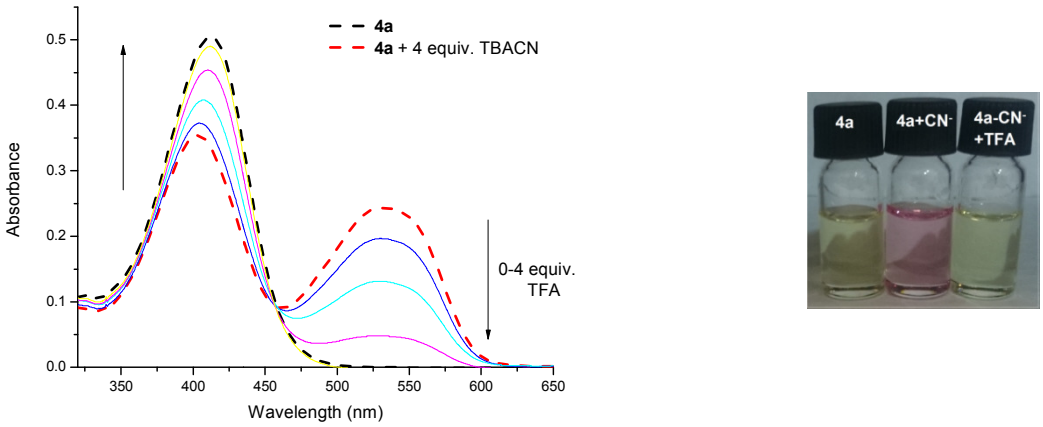

Fig. 46. Changes in the absorption spectra of **4a** (1×10^{-5} M in DMSO) in the presence of 4 equiv. of TBACN upon addition of increasing amount of TFA (0−4 equiv).

The experiment was performed with the other sensors **4b**, **4e**, **4f** and **4h**. The same result was obtained; i.e. the restoration of the probes and so the initial bands at 414, 413 and 413 nm for **4b**, **4e** and **4f**, respectively (Figs. A24-A26 in Annex 1). Except for **4h**, where only the band at 417 nm was recovered (Fig. 47). As mentioned before, it was reported that the two additional bands in the UV-vis spectrum belong to the keto-enamine tautomeric form of the molecule. Once the compound is dissolved in an acidic solution of DMSO, the phenol-imine tautomer is dominant, thus the bands of the other tautomer disappear and only the main band remains.

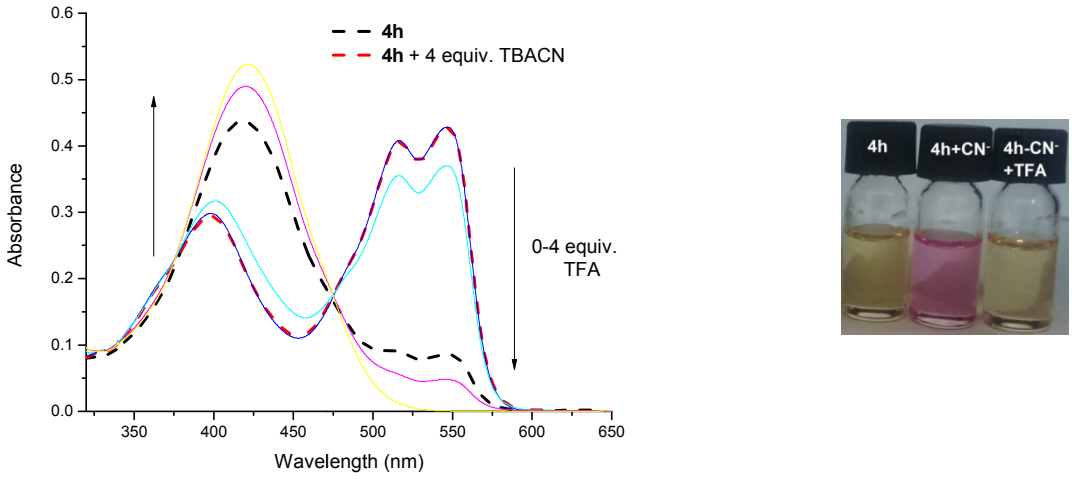

Fig. 47. Changes in the absorption spectra of **4h** (1×10^{-5} M in DMSO) in the presence of 4 equiv. of TBACN upon addition of increasing amount of TFA (0−4 equiv).

For chemosensor **4g**, in order to study the reversibility of the di-deprotonation process, increasing concentrations of TFA were added to a solution of **4g** in DMSO (1×10^{-5} M) containing 14 equiv. of cyanide, this caused a hypsochromic shift of 74 nm in the spectrum leading to the original band at 418 nm (Fig. 48, Scheme 22). The chemosensor was recovered after addition of 11 equiv. of TFA, and the light yellow color of the solution was restored (Photo; Fig. 45).

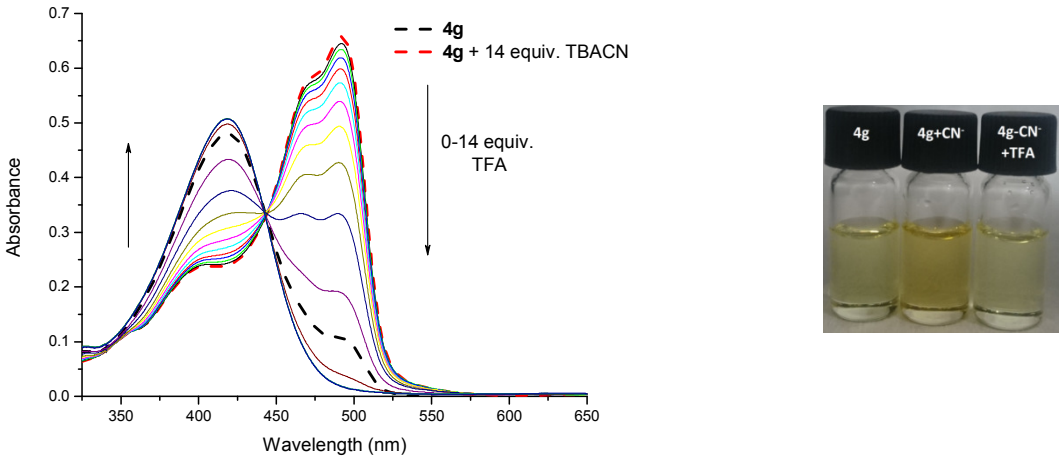

Fig. 48. Changes in the absorption spectra of **4g** (1×10^{-5} M in DMSO) in the presence of 14 equiv. of TBACN upon addition of increasing amount of TFA (0−14 equiv).

LOD and LOQ of the probes towards cyanide ion in aqueous medium

The limit of detection (LOD) and limit of quantification (LOQ) of cyanide anion were calculated from the fluorescence titration experiments in aqueous medium on the basis of the equations LOD = 3δ/S, LOQ = 10δ/S, where δ is the standard deviation of the response and S is the slope of the emission calibration curve of CN^- in DMSO/H_2O: 6/4 (v/v).[28]

Chemosensors **4a**, **4b** and **4g** showed the lowest LOD, 0.33 µM, 0.36 µM and 0.32 µM, respectively. Those results are much lower than the WHO guideline (2.7 µM) for cyanide[29], and also lower than LOD of CN^- in some of the recent reported publications.[20,30-32] Compound **4h** had a detection limit of 2.18 µM which is also lower than the WHO guidelines. Compounds **4e** and **4f** showed relatively higher LOD and LOQ compared to the others. The results obtained are summarized in Table 5.

Table 5. Values of LOD and LOQ of the chemosensors

	LOD (µM)	LOQ (µM)
4a	0.33	1.10
4b	0.36	1.21
4e	12.12	40.41
4f	6.08	20.27
4g	0.32	1.08
4h	2.18	7.27

Furthermore, the values of LOD and LOQ of **4g** with F^- and CN^- ions were also determined in DMSO from the UV-vis titration experiments (Figs. 49c, 49d). For cyanide: LOD = 1.69 µM, LOQ = 5.71 µM, and for fluoride: LOD = 1.89 µM, LOQ = 6.31 µM, and the LODs are both lower than the WHO guideline which are 0.07 mg/L (~ 2.7 µM) for cyanide, and 1.5 mg/L (~ 78.9 µM) for fluoride. It is worth noting that the detection limit of chemosensor **4g** is much better in aqueous media than in DMSO. Fig. 49 represents the emission calibration curves of **4a** and **4g** and the absorbance calibration curves of CN^- and F^- anions for compound **4g**. The other curves are grouped in Annex 1 (Fig. A27).

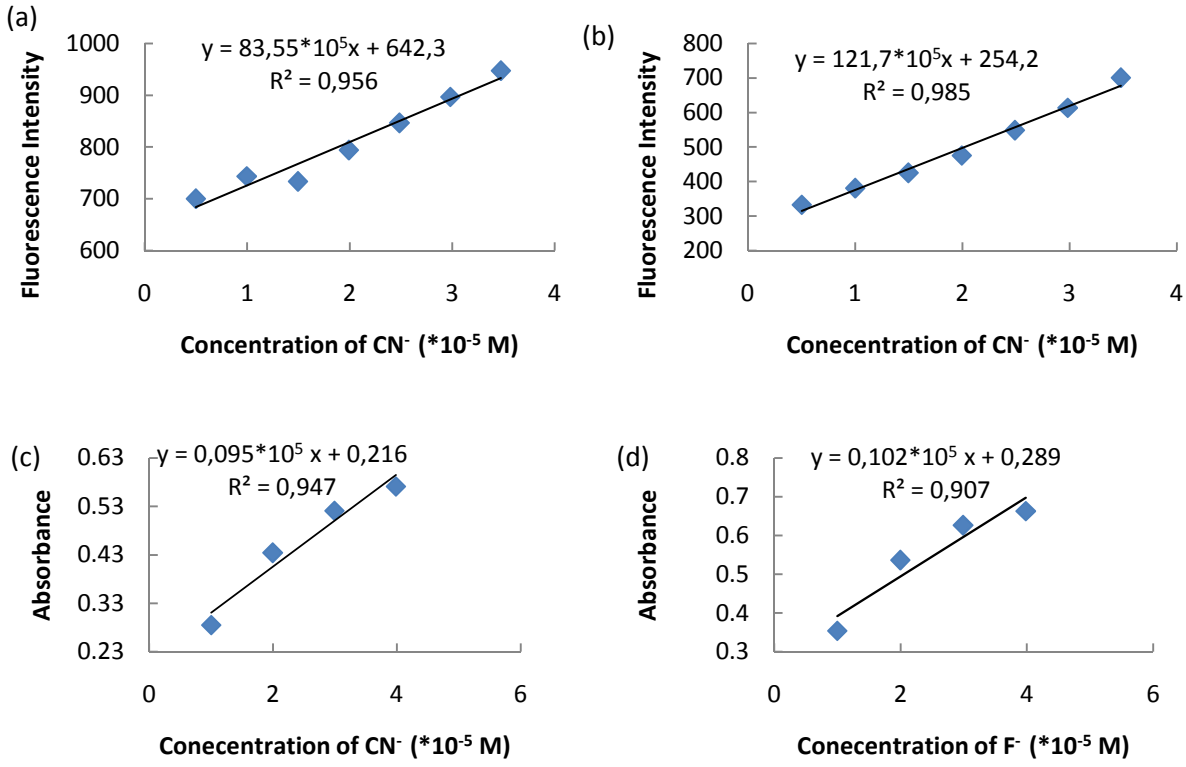

Fig. 49. The emission calibration curves of CN^- in DMSO/H_2O: 6/4 (v/v) for **4a** (a) and **4g** (b), and the absorbance calibration curves of CN^- (c) and F^- (d) in DMSO for **4g**.

Tap water experiment: Application as real life sensors

The good results obtained in DMSO/H_2O: 6/4 (v/v) for chemosensors **4a**, **4b**, **4e**, **4f** and **4g**, prompted us to put into practice the use of tap water instead of distilled water used so far in the precedent studies. Unlike distilled water, tap water contains a lot of components such as chlorine, fluoride and some salts of calcium, sodium, magnesium, etc. thus, making it a very competitive environment.

In this experiment KCN dissolved in tap water (5×10^{-3} M) was used instead of TBACN in DMSO and a fluorescence titration experiment was carried out. The results showed a turn-on in the fluorescence intensity with all tested chemosensors. Fig. 50 represents the response of probe **4a** and **4g** upon addition of 30 and 14 equivalents of KCN respectively, the photographs (from the insets) show a very clear fluorescence enhancement and prove that the detection of CN^- ions can be realized using a simple UV lamp without recourse to any other device. More results can be found in Annex 1 (Fig. A28).

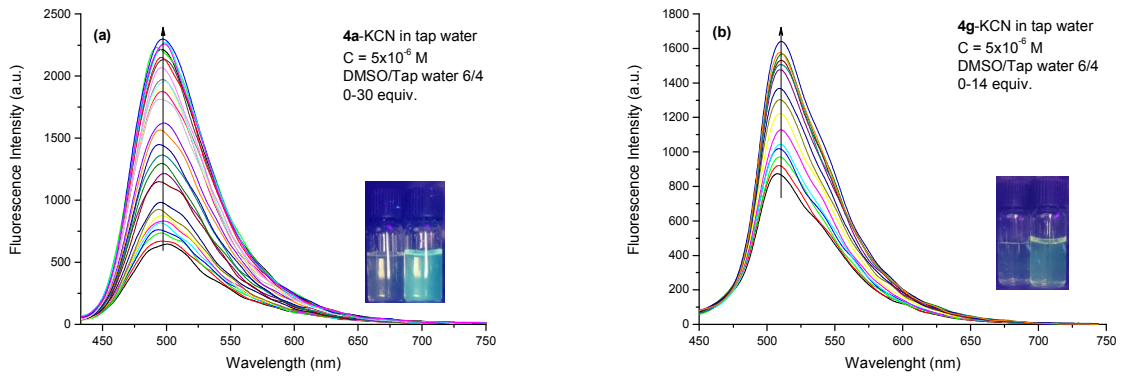

Fig. 50. Emission spectra of tap water experiment (5×10^{-6} M in DMSO/H_2O: 6/4) **4a** (a) and **4g** (b) upon addition of KCN dissolved in tap water. Insets: photographs of **4a** and **4g** (1×10^{-5} M) in DMSO/tap water (6/4, v/v) with KCN under UV lamp.

II.2. Theoretical Computation Results

To get further information about the effect of di-deprotonation on the geometries and electronic structures of **4g** and its complexes, with anions (**4g**+F^-, **4g**+AcO^-, **4g**+CN^- and **4g**+$H_2PO_4^-$), DFT and TD-DFT calculations were carried out using B3LYP functional[33] with dispersion correction and 631+g(d,p) basis set. The optimized geometries obtained in DMSO are illustrated in Fig. 51. The comparison of **4g** and complexes of its with anions (**4g**+F^-, **4g**+AcO^-, **4g**+CN^- and **4g**+$H_2PO_4^-$) gives the information that there is no any significant

structural changes after di-deprotonation. The calculated values of -179.8^{o} (0.05^{o}), -179.7^{o} (0.31^{o}), -179.7^{o} (0.24^{o}), -179.2^{o} (1.15^{o}), 178.9^{o} (-1.22^{o}) for the dihedral angles D1=C35-N39-C40-C41 (D2=N39-C40-C41-C42) for **4g**, **4g**+F^{-}, **4g**+AcO^{-}, **4g**+CN^{-} and **4g**+$H_2PO_4^{-}$, respectively, show that the planarity between thiophene and phenolic moiety does not change after di-deprotonation. The biggest changes in the dihedrals D1 and D2 are 0.9^{o} and 1.17^{o} for interaction with $H_2PO_4^{-}$. On the other hand, the bathochromic shifts seen in the absorption spectra after the interaction with anions can be explained with ICT changes. As shown in Table 6, and expected, the natural charges obtained from NBO calculations on O50 (-0.721e) and O51 (-0.709e) of **4g** become more negative after di-deprotonation.

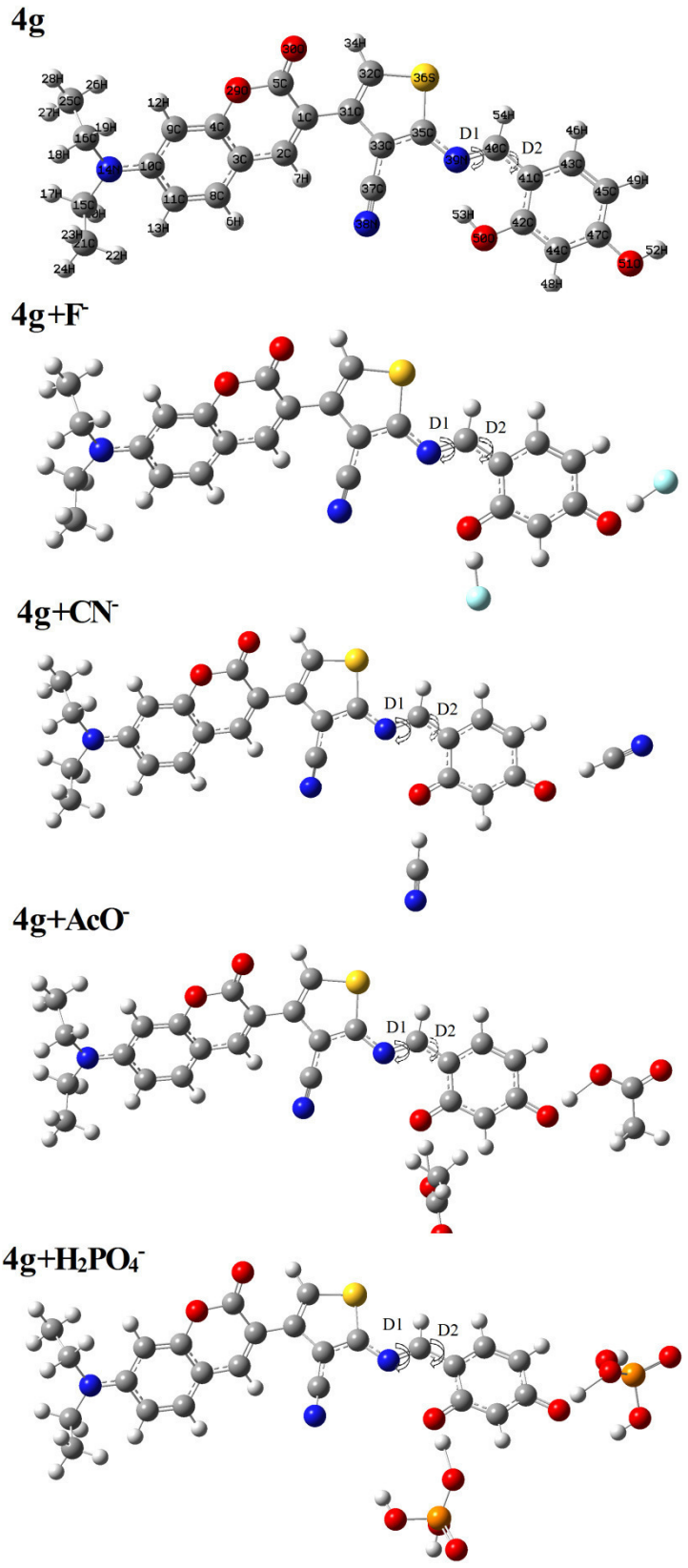

Fig. 51. The optimized structures of **4g**, **4g+F**$^-$, **4g+CN**$^-$, **4g+AcO**$^-$, and **4g+H$_2$PO$_4$**$^-$ in DMSO.

In addition, the same change is seen for the negative charge on the electron accepting cyano group. It can therefore be suggested that, according to these charge changes, the

complexes have a relatively better electron donation and also electron acceptance than the chemosensor **4g**. However, this leads to the relatively stronger ICT process which occurred from the dihydroxyphenyl part to cyano group after the di-deprotonation, which is responsible for the change in absorption spectra.

Table 6. The natural charge values (e) on O50, O51, and N38 atoms.

	4g	**4g+F^-**	**4g+CN^-**	**4g+AcO^-**	**4g+$H_2PO_4^-$**
O50	-0.721	-0.757	-0.746	-0.739	-0.767
O51	-0.709	-0.776	-0.779	-0.754	-0.751
N38	-0.385	-0.414	-0.421	-0.407	-0.396

To determine the photophysical properties theoretically, the absorption spectra of **4g**, **4g**+F^-, **4g**+AcO^-, **4g**+CN^- and **4g**+$H_2PO_4^-$ were calculated using TD-DFT/B3LYP/631+g(d,p) level in DMSO with PCM model.[34] The calculated absorption maximum wavelengths with the corresponding oscillator strengths (*f*) and absolute CI coefficients are given in Table 7. Chemosensor **4g** showed absorption maxima at 414 nm, which is in good agreement with the experimental value at 418 nm. With regards to **4g**+F^-, **4g**+AcO^-, **4g**+CN^- and **4g**+$H_2PO_4^-$, the absorption maxima exhibited bathochromic shift of 452 nm for **4g**+F^-, 462 nm for **4g**+CN^-, 453 nm for **4g**+AcO^-, and 462 nm for **4g**+$H_2PO_4^-$. These values correspond to the experimentally observed value of 492 nm. The values observed at about 440 nm for **4g**+CN^- and **4g**+$H_2PO_4^-$ correspond to the shoulder value at 468 nm given in the experimental data. The observed bathochromic shifts can be associated with the increased ICT transition, due to the interaction of **4g** with the anions *via* di-deprotonation of the phenolic protons, as discussed above.

Table 7. Calculated electronic excitation energies and corresponding oscillator strengths (*f*) with the absolute CI coefficients (percentage of the transition)

Molecules	λ_{max}(nm)	*f*	Transition	CI
4g	414	1.4055	HOMO-1→LUMO	0.41706 (35%)
			HOMO→LUMO+1	0.56365 (64%)
4g+F^-	452	1.0525	HOMO→LUMO	0.59340 (70%)
			HOMO→LUMO+1	0.37306 (28%)
4g+CN^-	462	0.8096	HOMO→LUMO	0.32325 (21%)
			HOMO→LUMO+1	0.62217 (77%)
			HOMO→LUMO	0.60942 (74%)

	444	0.6195	HOMO→LUMO+1	0.30674 (19%)
4g+ AcO⁻	453	0.7270	HOMO→LUMO HOMO→LUMO+1	0.67170 (90%) 0.20955 (9%)
4g+$H_2PO_4^-$	462	0.8897	HOMO→LUMO HOMO→LUMO+1	0.69595 (97%) 0.13279 (4%)
	440	0.6980	HOMO-1→LUMO HOMO→LUMO+1	0.32714 (21%) 0.61272 (75%)

The molecular orbitals related to the main absorption band for each structure are shown in Fig. 52 and Fig. A29 (in Annex 1) for only the most probable transitions. For chemosensor **4g**, its major contribution to the main peak comes from the transition HOMO→LUMO+1 at a percentage of 61%. The electron delocalization is over the coumarin and the thiophene moieties with the contribution of azomethine unit in HOMO, and is over the coumarin with a little contribution of the thiophene moiety in LUMO-1. After the di-deprotonation, the transitions related to the main peak are HOMO→LUMO for **4g+F⁻** (65%), **4g+AcO⁻** (90%), and **4g+$H_2PO_4^-$** (94%), and HOMO→LUMO+1 for **4g+CN⁻** (87%). The HOMO is delocalized over the entire units of the structure for **4g+F⁻**, **4g+AcO⁻**, and **4g+$H_2PO_4^-$**, while delocalization is over the entire units except for the coumarin moiety for **4g+CN⁻**. However, the delocalization is over the phenolic and cyanothiophene fragment through the azomethine unit for **4g+F⁻**, **4g+AcO⁻**, and **4g+$H_2PO_4^-$** and, **4g+CN⁻**. According to these results, the electron density on the phenolic part increases after the di-deprotonation. These results are said to relate to the increased ICT as a result of the increased electron density after the di-deprotonation of chemosensor **4g**.

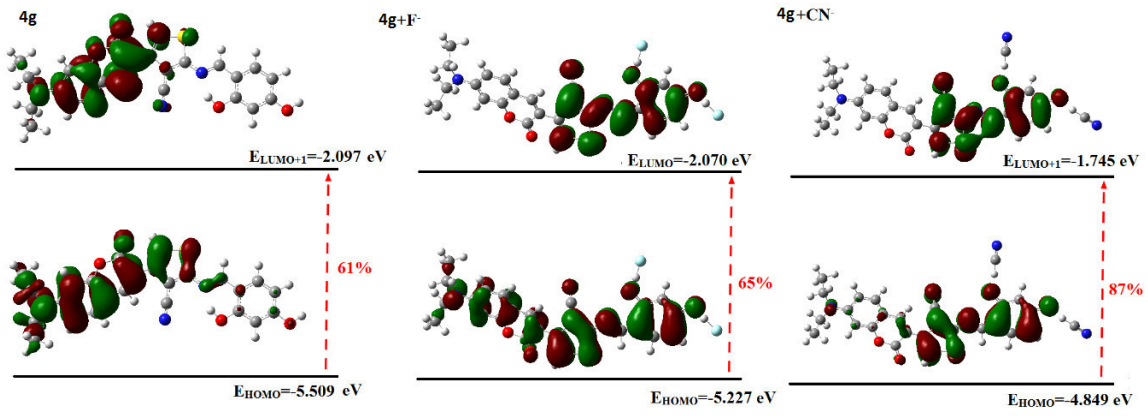

Fig. 52. The optimized structures of **4g**, **4g+F⁻** and **4g+CN⁻** obtained using DFT/B3LYP/631+g(d,p) level.

Conclusion

Compounds **4a-h** were chosen for anion interaction due to their excellent photophysical properties and their good absorbtion in the visible region. The sensing abilities of sensors **4** were tested in DMSO and in DMSO/H_2O (6/4, v/v) solutions with ten different anions. Upon addition of 1 equiv. of each anion in organic medium, only CN^-, F^- and AcO^- induced distinct spectrum changes while other anions showed either no or slight changes in the absorption spectra relative to the free receptors **4** and reduced the main band to some extent. Consistently with the changes of UV-vis spectra, the solutions' color of **4** in the presence of CN^-, F^- and AcO^- ions changed from yellow to red (from yellow to orange for **4g**). An exception was observed with compound **4d**. Compound **4g** showed a "naked-eye" selectivity towards fluoride after addition of 14 equivalents.

When 40% of water was introduced into the system, the detection shifted to CN^- with no interference from the other anions, indicating that receptors **4a**, **4b**, **4e**, **4f**, **4g** and **4h** can serve as potential chemosensors for CN^- anion in aqueous medium. The stoichiometry of the interaction **4g**-CN^- was determined as 1:1 using Job's plot experiment and was confirmed by ^1H NMR titrations and theoretical calculations as a di-deprotonation of the OH protons. The rest of the probes interacted *via* deprotonation of the OH proton and addition to the C=N double bond. The spectral changes accompanied by the addition of anions are attributed to an increase of the ICT efficiency of the molecules. The LODs of the probes for cyanide were calculated, and were lower than the WHO guidelines for compounds **4a**, **4b**, **4g** and **4h**.

The reversibility and applicability of the probes were also investigated. The results indicate that the receptors could be recycled simply through treatment with TFA. For the practical application, tap water experiments were carried out. The results showed that receptors **4a**, **4b**, **4e**, **4f** and **4g** could have a practical application for detection of CN^- anion in environmental samples.

This study shows clearly that a donor group in the 4-position of the salicylidene moiety influences dramatically the sensing ability of these compounds; this is illustrated by compounds **4c** and **4d**. Finally, it is worth noting that except for compound **4g**, the detection of CN^- by the other probes was rather fluorescent.